9
Skyrmions

9.1 The Skyrme model

The Skyrme model [377, 379] is a nonlinear theory of pions in three spatial dimensions, with the Skyrme field, $U(t,\mathbf{x})$, being an $SU(2)$-valued scalar. Although not involving quarks, it can be regarded as an approximate, low energy effective theory of QCD, becoming exact as the number of quark colours becomes large [428]. Remarkably, and this was Skyrme's main motivation for constructing and studying this model, it has topological soliton solutions that can be interpreted as baryons. These solitons are called Skyrmions.

The model is defined by the Lagrangian

$$L = \int \left\{ \frac{F_\pi^2}{16} \mathrm{Tr}(\partial_\mu U \partial^\mu U^\dagger) + \frac{1}{32e^2} \mathrm{Tr}([\partial_\mu U U^\dagger, \partial_\nu U U^\dagger][\partial^\mu U U^\dagger, \partial^\nu U U^\dagger]) \right\} d^3x , \quad (9.1)$$

where F_π and e are parameters, whose values are fixed by comparison with experimental data. These parameters can be scaled away by using energy and length units of $F_\pi/4e$ and $2/eF_\pi$ respectively, which we adopt from now on. In terms of these standard units the Skyrme Lagrangian can be written as

$$L = \int \left\{ -\frac{1}{2} \mathrm{Tr}(R_\mu R^\mu) + \frac{1}{16} \mathrm{Tr}([R_\mu, R_\nu][R^\mu, R^\nu]) \right\} d^3x , \quad (9.2)$$

where we have introduced the $su(2)$-valued current $R_\mu = (\partial_\mu U)U^\dagger$. The Euler-Lagrange equation which follows from (9.2) is the Skyrme field equation

$$\partial_\mu \left(R^\mu + \frac{1}{4}[R^\nu, [R_\nu, R^\mu]] \right) = 0 , \quad (9.3)$$

which is a nonlinear wave equation for $U(t,\mathbf{x})$. An interesting feature of (9.3) is that it is in the form of a current conservation equation $\partial_\mu \tilde{R}^\mu = 0$, where $\tilde{R}^\mu = R^\mu + \frac{1}{4}[R^\nu,[R_\nu,R^\mu]]$.

One imposes the boundary condition $U(\mathbf{x}) \to 1_2$ as $|\mathbf{x}| \to \infty$. The vacuum, the unique field of minimal energy, is then $U(\mathbf{x}) = 1_2$ for all $\mathbf{x}$.

The Skyrme Lagrangian has an $(SU(2) \times SU(2))/\mathbb{Z}_2 \cong SO(4)$ chiral symmetry corresponding to the transformations $U \mapsto \mathcal{O}_1 U \mathcal{O}_2$, where $\mathcal{O}_1$ and $\mathcal{O}_2$ are constant elements of $SU(2)$. However, the boundary condition $U(\infty) = 1_2$ spontaneously breaks this chiral symmetry to an $SO(3)$ isospin symmetry given by the conjugation

$$U \mapsto \mathcal{O} U \mathcal{O}^\dagger, \qquad \mathcal{O} \in SU(2). \tag{9.4}$$

In order to make explicit the nonlinear pion theory, we write

$$U = \sigma + i\boldsymbol{\pi} \cdot \boldsymbol{\tau}, \tag{9.5}$$

where $\boldsymbol{\tau}$ denotes the triplet of Pauli matrices, $\boldsymbol{\pi} = (\pi_1, \pi_2, \pi_3)$ is the triplet of pion fields and σ is an additional field determined by the pion fields through the constraint $\sigma^2 + \boldsymbol{\pi} \cdot \boldsymbol{\pi} = 1$, which is required since $U \in SU(2)$. Not only the magnitude, but also the sign of σ may be regarded as determined by the requirement of continuity of the field, and the boundary conditions $\boldsymbol{\pi}(\infty) = 0$, $\sigma(\infty) = 1$. In terms of the pion fields, an isospin transformation is $\boldsymbol{\pi} \mapsto M\boldsymbol{\pi}$, where M is the $SO(3)$ matrix corresponding to the $SU(2)$ matrix $\mathcal{O}$.

$$M_{ij} = \frac{1}{2}\mathrm{Tr}(\tau_i \mathcal{O} \tau_j \mathcal{O}^\dagger). \tag{9.6}$$

Pion particles arise from the quantization of small fluctuations of the pion field around the vacuum $\boldsymbol{\pi} = \mathbf{0}$, $\sigma = 1$. Note that substituting (9.5) into the Lagrangian (9.2) reveals that the pions are massless. They are the Goldstone bosons of the spontaneously broken chiral symmetry. An additional term

$$L_{\text{mass}} = m_\pi^2 \int \mathrm{Tr}(U - 1_2)\, d^3x \tag{9.7}$$

can be included in the Lagrangian of the Skyrme model and gives the pions a (tree-level) mass m_π. As most of our discussion is independent of this extra term we do not include it at this stage, but in Section 9.9 we address the modifications that it generates.

If one restricts to static fields, $U(\mathbf{x})$, then the Skyrme energy functional derived from the Lagrangian (9.2) is

$$E = \frac{1}{12\pi^2} \int \left\{ -\frac{1}{2}\mathrm{Tr}(R_i R_i) - \frac{1}{16}\mathrm{Tr}([R_i,R_j][R_i,R_j]) \right\} d^3x, \tag{9.8}$$

where we have introduced the additional factor of $1/12\pi^2$ for later convenience. Static solutions of the Skyrme field equation (9.3) are therefore critical points (either minima or saddle points) of this energy.

At first sight U, at a fixed time, is a map from $\mathbb{R}^3$ into S^3, the group manifold of $SU(2)$. However, the boundary condition implies a one-point compactification of space, so that topologically $U : S^3 \mapsto S^3$, where the domain S^3 is to be identified with $\mathbb{R}^3 \cup \{\infty\}$. As discussed in Chapter 3 the homotopy group $\pi_3(S^3)$ is $\mathbb{Z}$, which implies that maps between 3-spheres fall into homotopy classes indexed by an integer, which we denote by B. This integer is also the degree of the map U and has the explicit representation

$$B = -\frac{1}{24\pi^2}\int \varepsilon_{ijk}\mathrm{Tr}\,(R_iR_jR_k)\,d^3x\,, \tag{9.9}$$

where $R_i = (\partial_i U)U^\dagger$, as before. As B is a topological invariant, it is conserved under continuous deformations of the field, including time evolution. It is this conserved topological charge which Skyrme identified with baryon number. B is the principal property of a Skyrmion.

The presence of a topological charge is, by itself, not sufficient to ensure the existence of stable topological solitons since we also need to evade Derrick's theorem [107]. But note that the static Skyrme energy decomposes into two components, $E = E_2 + E_4$, corresponding to the terms which are quadratic and quartic in spatial derivatives of the Skyrme field. Under a rescaling of the spatial coordinates $\mathbf{x} \mapsto \mu\mathbf{x}$, the energy becomes

$$e(\mu) = \frac{1}{\mu}E_2 + \mu E_4\,. \tag{9.10}$$

The two terms therefore scale in opposite ways, leading to a minimal value of $e(\mu)$ for a finite $\mu \neq 0$. This implies that any soliton will have a well defined scale and will neither expand to cover all of space nor contract to be localized at a single point. Note that for any static solution, and in particular for a Skyrmion, which is the minimal energy configuration in a given topological sector, $e(\mu)$ must take its minimal value when $\mu = 1$, so the energy contributions from the quadratic and quartic terms are exactly equal. From this discussion it is clear why the sigma model (the Lagrangian consisting of only the first term in (9.2)) does not support stable solitons. This problem is cured by the addition of the second term in (9.2), known as the Skyrme term. Clearly any term which is of degree 4 or higher in the spatial derivatives would do equally well in this respect, but the Skyrme term is the unique expression of degree 4 which is Lorentz invariant and for which the resulting field equation remains second order in the time derivative.

A more geometrical description of the static Skyrme energy exists [282], which is useful in several contexts. As in nonlinear elasticity theory, the energy density of a Skyrme field depends on the local stretching associated with the map $U : \mathbb{R}^3 \mapsto S^3$. For this formulation, let us introduce the strain tensor D_{ij}, defined at each point $\mathbf{x} \in \mathbb{R}^3$ by

$$D_{ij} = -\frac{1}{2}\mathrm{Tr}(R_i R_j)\,, \tag{9.11}$$

which is a symmetric, positive definite 3×3 matrix, and which can be thought of as quantifying the deformation induced by the map U. The image under U of an infinitesimal sphere of radius ε and centre $\mathbf{x}$ in $\mathbb{R}^3$, to leading order in ε, is an ellipsoid with principal axes $\varepsilon\lambda_1, \varepsilon\lambda_2, \varepsilon\lambda_3$, where λ_1^2, λ_2^2, λ_3^2 are the three non-negative eigenvalues of the matrix D_{ij}. The signs of λ_1, λ_2 and λ_3 are chosen so that $\lambda_1\lambda_2\lambda_3$ is positive (negative) if U is locally orientation preserving (reversing). In terms of these eigenvalues, the static energy E, and baryon number B, can be computed as integrals over $\mathbb{R}^3$ of the corresponding densities $\mathcal{E}$ and $\mathcal{B}$ given by

$$\mathcal{E} = \frac{1}{12\pi^2}(\lambda_1^2+\lambda_2^2+\lambda_3^2+\lambda_1^2\lambda_2^2+\lambda_2^2\lambda_3^2+\lambda_3^2\lambda_1^2)\,, \quad \mathcal{B} = \frac{1}{2\pi^2}\lambda_1\lambda_2\lambda_3\,. \tag{9.12}$$

From the simple inequality

$$(\lambda_1 \pm \lambda_2\lambda_3)^2 + (\lambda_2 \pm \lambda_3\lambda_1)^2 + (\lambda_3 \pm \lambda_1\lambda_2)^2 \geq 0\,, \tag{9.13}$$

it follows from the formulae (9.12) that $\mathcal{E} \geq |\mathcal{B}|$ and therefore the Skyrme energy satisfies the Faddeev-Bogomolny lower bound [126]

$$E \geq |B|\,. \tag{9.14}$$

In contrast to monopoles and vortices, this bound can not be saturated for any non-trivial (i.e. $B \neq 0$) finite energy configuration. This is because the bound is attained only when all the eigenvalues of the strain tensor have modulus 1 at all points in space – an isometry – and this is obviously not possible since $\mathbb{R}^3$ is not isometric to S^3. Note that the bound can be attained if the spatial domain is taken to be the 3-sphere of unit radius: we discuss this further in Section 9.9.

After the baryon number and energy, the most significant characteristic of a static solution of the Skyrme equation is its asymptotic field, which satisfies the linearized form of the equation. To leading order, the three components of the pion field $\boldsymbol{\pi}$ each obey Laplace's equation, and σ can be taken to be unity. More precisely, $\boldsymbol{\pi}$ has a multipole expansion, in which each term is an inverse power of $r = |\mathbf{x}|$, say $r^{-(l+1)}$, times a triplet of angular functions. The leading term, with the smallest l, obeys Laplace's equation, whereas subleading terms may not, because of the

nonlinear aspect of the Skyrme equation. For the leading term, therefore, the angular functions are a triplet of linear combinations of the spherical harmonics $Y_{l,m}(\theta,\varphi)$, with m taking integer values in the range $-l \leq m \leq l$. These spherical harmonics can also be expressed in Cartesian coordinates, which often gives more convenient and elegant formulae for the asymptotic fields.

One of the few precise results concerning the Skyrme equation (9.3) is that this multipole expansion can not lead with a monopole term, with $l = 0$. The leading term is a dipole or higher multipole. The proof is as follows [286]. For a static field, the equation implies that the spatial current

$$\tilde{R}_i = R_i + \frac{1}{4}[R_j, [R_j, R_i]] \tag{9.15}$$

has zero divergence and no singularity. Therefore the flux of $\tilde{R}_i$ through a large sphere of radius R (centred at the origin) vanishes, that is,

$$\int_{S^2_R} \tilde{R}_i n^i \, dS = 0\,, \tag{9.16}$$

where n^i is the unit outward normal. Now, in the asymptotic region, $\tilde{R}_i$ can be replaced by R_i, which in turn simplifies to $i(\partial_i \boldsymbol{\pi}) \cdot \boldsymbol{\tau}$. For a monopole asymptotic field,

$$\boldsymbol{\pi} = \frac{\mathbf{c}}{r} \tag{9.17}$$

where $\mathbf{c}$ is a constant vector, so $\tilde{R}_i$ has the leading asymptotic behaviour $-i\mathbf{c} \cdot \boldsymbol{\tau} x_i / r^3$. Then $\tilde{R}_i n^i = -i\mathbf{c} \cdot \boldsymbol{\tau}/r^2$, so the flux through the sphere is $-4\pi i \mathbf{c} \cdot \boldsymbol{\tau}$. This vanishes only if $\mathbf{c} = \mathbf{0}$.

Recently, it has been rigorously proved [294] that for any non-vacuum solution of the Skyrme equation, the multipole expansion is non-trivial. In other words, the pion field does not vanish to all orders in l, and the leading term is a multipole satisfying the Laplace equation.

9.2 Hedgehogs

Esteban [123] has proved the existence of a $B = 1$ Skyrmion, that is, a minimizer of the energy functional (9.8) within the charge 1 sector, following earlier work of Kapitansky and Ladyzenskaia [230] in which it was proved that a minimizer exists within the family of spherically symmetric charge 1 Skyrme fields. It is believed to be true, though not yet proven, that these two minimizers are the same, that is, the minimal energy Skyrmion in the $B = 1$ sector is spherically symmetric. Here, spherically symmetric does not mean that the Skyrme field is just a function of the radial coordinate r, since it is easily seen that such a field

must have $B = 0$. When we refer to a spatial symmetry of a Skyrmion, such as spherical symmetry, we mean that the field has the equivariance property that the effect of a spatial rotation can be compensated by an isospin transformation (9.4). This implies that both the energy density $\mathcal{E}$, and baryon density $\mathcal{B}$, are strictly invariant under the symmetry.

The spherically symmetric $B = 1$ Skyrmion was presented in the original work of Skyrme and takes the hedgehog form (cf. Section 4.3)

$$U(\mathbf{x}) = \exp\{if(r)\hat{\mathbf{x}} \cdot \boldsymbol{\tau}\} \equiv U_{\mathrm{H}}(\mathbf{x}). \tag{9.18}$$

In terms of $\boldsymbol{\pi}$ and σ fields,

$$\boldsymbol{\pi} = \cos f(r)\,\hat{\mathbf{x}}, \quad \sigma = \sin f(r). \tag{9.19}$$

The name hedgehog derives from the fact that the pion fields of this configuration point radially outward from the origin at all points in space, so $\hat{\boldsymbol{\pi}} = \hat{\mathbf{x}}$. f is a real radial profile function with the boundary conditions $f(0) = \pi$ and $f(\infty) = 0$. The latter condition ensures that $U(\infty) = 1_2$, while the former guarantees that $U(0)$ is well defined and that $B = 1$. The value of B is confirmed by substituting the hedgehog ansatz into the expression (9.9) for the baryon number, giving

$$B = -\frac{2}{\pi}\int_0^\infty f' \sin^2 f \, dr = \frac{1}{\pi} f(0) = 1. \tag{9.20}$$

Alternatively, we can easily verify that if f monotonically decreases, then each point of the target space $SU(2)$ (except $U = 1_2$) has exactly one preimage in $\mathbb{R}^3$, with positive Jacobian.

Substituting the hedgehog ansatz (9.18) into the static Skyrme equation yields the second order nonlinear ordinary differential equation

$$(r^2 + 2\sin^2 f)f'' + 2rf' + \sin 2f \left(f'^2 - 1 - \frac{\sin^2 f}{r^2}\right) = 0. \tag{9.21}$$

The solution of this equation, satisfying the boundary conditions, can not be obtained in closed form but it is a simple task to compute it numerically using a shooting method. The numerical solution is presented in Fig. 9.1.

The energy, given by

$$E = \frac{1}{3\pi}\int_0^\infty \left\{r^2 f'^2 + 2\sin^2 f\,(1 + f'^2) + \frac{\sin^4 f}{r^2}\right\} dr, \tag{9.22}$$

is calculated to be $E = 1.232$, to three decimal places, and so the $B = 1$ Skyrmion exceeds the Faddeev-Bogomolny bound by approximately 23%.

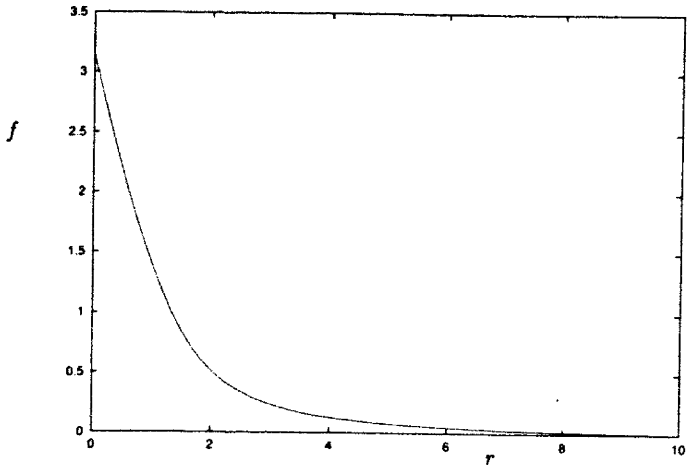

Fig. 9.1. The profile function $f(r)$ for the $B = 1$ Skyrmion.

The Skyrmion described by (9.18) is located at the origin, but it can be positioned at any point in space and given any orientation by acting with the translation and rotation groups of $\mathbb{R}^3$. The moduli space of charge 1 Skyrmions is therefore six-dimensional. In general, it is to be expected that the moduli space of a charge B Skyrmion is nine-dimensional, since in addition to translations and rotations there is also the action of the three-dimensional isospin group (9.4). However, for $B = 1$, an isospin transformation is equivalent to a spatial rotation, which is of course why the Skyrmion is spherically symmetric, so three moduli are lost.

A linearization of Eq. (9.21) reveals the large r asymptotic behaviour of the profile function, $f \sim C/r^2$, for some constant C, which numerically is found to be $C = 2.16$. Therefore, the leading order asymptotic fields are

$$\pi = \frac{C}{r^2}\hat{\mathbf{x}}, \quad \sigma = 1. \tag{9.23}$$

In other words, from far away a single Skyrmion resembles a triplet of orthogonal pion dipoles, with dipole strength $4\pi C$. In Section 9.3 we discuss the asymptotic interactions of well separated Skyrmions, and their interpretation in terms of dipole-dipole forces.

There are further solutions involving the hedgehog ansatz (9.18). Note that U is well defined provided $f(0) = k\pi$, where $k \in \mathbb{Z}$, and a glance at Eq. (9.20) shows that the field in this case describes a spherically symmetric configuration with $B = k$. The pion field still points radially, but inwards or outwards. There appear to be solutions of the equation for the profile function for all values of k [379, 220]. Solutions have been

constructed numerically for several values. The $k = -1$ solution is the antiSkyrmion, whose profile function is obtained from that of the Skyrmion by the replacement $f \mapsto -f$. For $|k| > 1$ these hedgehog solutions do not represent the minimal energy Skyrmions with $B = k$, and in fact these solutions are not even bound against break-up into $|k|$ well separated Skyrmions (or antiSkyrmions if $k < 0$). For example, the $k = 2$ hedgehog has an energy $E = 3.67 > 1.232 \times 2$, and has been shown to have six unstable modes. The hedgehog solutions, for $|k| > 1$, are therefore almost certainly all unstable, saddle points of the energy.

A rigorous proof of the existence of charge B, minimal energy Skyrmions with $|B| > 1$ appears to be difficult, and has not yet been found. Their existence has been established by Esteban [123], but only under the assumption that

$$E_B < E_{B'} + E_{B-B'}\,, \tag{9.24}$$

for all $B' \in \mathbb{Z} - \{0, B\}$, where $E_{B'}$ denotes the infimum of the energy (9.8) within the space of Skyrme fields with baryon number B'. Esteban [123] was able to prove the weaker inequality

$$E_B \leq E_{B'} + E_{B-B'}\,, \tag{9.25}$$

but the strict inequality is not yet proved in general. The strict inequality would prevent the break-up of a charge B field into infinitely separated clusters of charge B' and $B - B'$, and would imply that the energy E_B was attained by a Skyrmion solution. In the following section we present a physical perspective on these inequalities, in terms of the forces between well separated Skyrmions. Later, we will also describe the solutions that have been discovered numerically, that are believed to be the minimal energy Skyrmions.

9.3 Asymptotic interactions

As noted above, the asymptotic field of a single Skyrmion is that of a triplet of orthogonal dipoles and we can make use of this interpretation to calculate the asymptotic forces between two well separated Skyrmions by computing the interaction energy of the pair of dipole triplets. It is convenient to rewrite (9.23) in the form

$$\pi_j = \frac{C}{r^2}\hat{x}^j = \frac{\mathbf{p}_j \cdot \mathbf{x}}{4\pi r^3}\,, \tag{9.26}$$

where we have introduced the three orthogonal dipole moments

$$\mathbf{p}_j = 4\pi C \mathbf{e}_j\,. \tag{9.27}$$

with $\{\mathbf{e}_j\}$ being the standard basis vectors of $\mathbb{R}^3$. More generally, the frame of dipoles may be rotated, but their magnitudes are unchanged. With the energy normalized as in (9.8) the interaction energy of two individual dipoles, with moments $\mathbf{p}, \mathbf{q}$ and relative position vector $\mathbf{X}$, is given by

$$E_{\text{dip}} = \frac{1}{24\pi^3}(\mathbf{p}\cdot\tilde{\partial})(\mathbf{q}\cdot\tilde{\partial})\frac{1}{|\mathbf{X}|}, \tag{9.28}$$

where $\tilde{\partial}_i = \frac{\partial}{\partial X^i}$. This is similar to the formula for the interaction energy of two electric dipoles, but has the opposite sign, because the pion field is a scalar, so like charges attract.

We can use the translation and isospin symmetries to position the first Skyrmion at the origin in standard orientation, and the second Skyrmion at the point $\mathbf{X} \in \mathbb{R}^3$, with $X = |\mathbf{X}| \gg 1$, and with an orientation determined by the $SU(2)$ matrix $\mathcal{O}$. The dipole moments of the second Skyrmion are then $\mathbf{q}_j = M\mathbf{p}_j$, where M is the $SO(3)$ matrix corresponding to $\mathcal{O}$, as given in (9.6). There is a dipole interaction between $\mathbf{p}_j$ and $\mathbf{q}_k$ only if $j = k$, so summing the interactions of the three pairs and using (9.28) we obtain the total interaction energy

$$E_{\text{int}} = \frac{2C^2}{3\pi}(\tilde{\boldsymbol{\partial}}\cdot M\tilde{\boldsymbol{\partial}})\frac{1}{X}. \tag{9.29}$$

To get a better understanding of this, we can reexpress the matrix M in terms of a rotation through an angle ψ about an axis $\hat{\mathbf{n}}$.

$$M_{ij} = \cos\psi\,\delta_{ij} + (1-\cos\psi)\hat{n}_i\hat{n}_j + \sin\psi\,\varepsilon_{ijk}\hat{n}_k. \tag{9.30}$$

The interaction energy (9.29) then takes the form

$$E_{\text{int}} = -\frac{2C^2}{3\pi}(1-\cos\psi)\frac{1-3(\hat{\mathbf{X}}\cdot\hat{\mathbf{n}})^2}{X^3}. \tag{9.31}$$

Clearly, by a suitable choice of the axis $\hat{\mathbf{n}}$, the two Skyrmions can be made to either repel or attract, corresponding to a positive or negative interaction energy respectively. The attraction is maximal (that is, the interaction energy is minimal) if $\hat{\mathbf{X}}\cdot\hat{\mathbf{n}} = 0$ and $\psi = \pi$, in other words, one Skyrmion is rotated relative to the other through an angle of 180° about a line perpendicular to the line joining them. This is known as the attractive channel. Note that in making this statement we are using the fact that an isospin rotation of a single Skyrmion is equivalent to a spatial rotation, so we may think in terms of the latter.

In Section 9.8, where we discuss Skyrmion dynamics, we return to formula (9.31) in relation to setting up initial conditions for several well separated Skyrmions such that they mutually attract.

The dipole calculation described above can not serve as a rigorous derivation of the asymptotic interaction energy of two Skyrmions since it assumes that a Skyrmion whose field is asymptotically of the dipole triplet form also reacts to an external field like a dipole triplet. Below we present a more formal calculation of the interaction energy, closely following the presentation in [365], which confirms the result obtained from the dipole picture.

In Eq. (9.8) we have expressed the static energy in terms of the right currents $R_i = \partial_i U U^\dagger$, but we could also have chosen to write it in terms of the left currents $L_i = U^\dagger \partial_i U$, giving an identical expression after the replacement of R_k by L_k. These two equivalent formulations are useful in what follows, as are the quantities $\tilde{R}_i$ and $\tilde{L}_i$ defined as

$$\tilde{R}_i = R_i - \frac{1}{4}[R_j, [R_j, R_i]]\,, \quad \tilde{L}_i = L_i - \frac{1}{4}[L_j, [L_j, L_i]]\,. \tag{9.32}$$

It follows from the Skyrme field equation (9.3) that for a static solution, both these currents are divergenceless, that is,

$$\partial_i \tilde{R}_i = \partial_i \tilde{L}_i = 0\,. \tag{9.33}$$

To calculate the interaction energy of two well separated Skyrmions we use the product ansatz of two hedgehog fields

$$U = U^{(1)} U^{(2)}\,, \quad U^{(1)} = U_{\rm H}(\mathbf{x})\,, \quad U^{(2)} = \mathcal{O} U_{\rm H}(\mathbf{x} - \mathbf{X}) \mathcal{O}^\dagger\,. \tag{9.34}$$

In computing the energy of the product field (9.34) it is helpful to note the following relation

$$L_i = U^\dagger \partial_i U = U^{(2)\dagger}(L_i^{(1)} + R_i^{(2)}) U^{(2)}\,, \tag{9.35}$$

where $L_i^{(1)}$ denotes the left current constructed from the field $U^{(1)}$, and so on. Substituting this expression into the Skyrme energy gives a term involving only $L_i^{(1)}$, one involving only $R_i^{(2)}$ and a cross term. The first two terms each contribute precisely the energy of a single Skyrmion and the cross term gives the interaction energy which, neglecting terms that are quadratic in both $L_i^{(1)}$ and $R_i^{(2)}$, has the leading order contribution

$$E_{\rm int} \sim -\frac{1}{12\pi^2} \int_{\mathbb{R}^3} {\rm Tr}(L_i^{(1)} \tilde{R}_i^{(2)} + \tilde{L}_i^{(1)} R_i^{(2)} - L_i^{(1)} R_i^{(2)})\, d^3x\,. \tag{9.36}$$

In order to evaluate this integral for large X, we divide $\mathbb{R}^3$ into three regions, I, II and III, given by $I = \{\mathbf{x} : |\mathbf{x}| < \rho\}$, $II = \{\mathbf{x} : |\mathbf{x} - \mathbf{X}| < \rho\}$ and $III = \mathbb{R}^3 - I - II$, with $2\rho < X$. For large X we choose ρ large enough so that outside region I we can apply the asymptotic expression

$$L_i^{(1)} \sim l_i^{(1)} \equiv iC\partial_i \Big(\frac{\mathbf{x} \cdot \boldsymbol{\tau}}{|\mathbf{x}|^3} \Big)\,, \tag{9.37}$$

and similarly outside region II

$$R_i^{(2)} \sim r_i^{(2)} \equiv iC\partial_i \left(\frac{\mathcal{O}(\mathbf{x}-\mathbf{X}) \cdot \tau \mathcal{O}^\dagger}{|\mathbf{x}-\mathbf{X}|^3} \right). \tag{9.38}$$

Note that since $\tilde{L}_i^{(1)}$ differs from $L_i^{(1)}$ only by a triple product of $L_i^{(1)}$'s (and similarly for $\tilde{R}_i^{(2)}$) then in the above limits we also have that

$$\tilde{L}_i^{(1)} \sim l_i^{(1)} \quad \text{and} \quad \tilde{R}_i^{(2)} \sim r_i^{(2)}. \tag{9.39}$$

Furthermore, we also require that ρ is small enough that $l_i^{(1)}$ may be taken to be constant over region II and $r_i^{(2)}$ constant over region I. This is achieved by letting $\rho \to \infty$ as $X \to \infty$ in such a way that $\rho/X \to 0$. Substituting these approximations into (9.36) we arrive at

$$\begin{aligned} E_{\text{int}} \sim & -\frac{1}{12\pi^2} \mathrm{Tr} \Big\{ r_i^{(2)}\Big|_{\mathbf{x}=\mathbf{0}} \int_I (\tilde{L}_i^{(1)} - l_i^{(1)})\, d^3x \\ & + l_i^{(1)}\Big|_{\mathbf{x}=\mathbf{X}} \int_{II} (\tilde{R}_i^{(2)} - r_i^{(2)})\, d^3x + \int_{\mathbb{R}^3} l_i^{(1)} r_i^{(2)}\, d^3x \Big\}. \end{aligned} \tag{9.40}$$

Expanding $\tilde{L}_i^{(1)}$ in terms of Pauli matrices as

$$\tilde{L}_i^{(1)} = i\tilde{L}_{im}\tau_m, \tag{9.41}$$

we see from Eq. (9.33) that for each $m = 1, 2, 3$, $\tilde{L}_{im}$ are the components of a divergenceless vector field, which implies that there exists a potential Z_{km} such that

$$\tilde{L}_{im} = \varepsilon_{ijk}\partial_j Z_{km}. \tag{9.42}$$

Explicitly, it can be checked that this potential is given by

$$Z_{km} = \left(\sin^2 f - \frac{\sin^4 f}{r^2} \right) \hat{x}_k \hat{x}_m + \frac{rf'}{2} \left(1 + 2\frac{\sin^2 f}{r^2} \right) \varepsilon_{kmn}\hat{x}_n. \tag{9.43}$$

Thus

$$\begin{aligned} \int_I \tilde{L}_i^{(1)}\, d^3x &= i\tau_m \int_{\partial I} \varepsilon_{ijk} Z_{km} \hat{x}_j\, dS \\ &= i\tau_m \int_{\partial I} (\delta_{im} - \hat{x}_i\hat{x}_m) \frac{rf'}{2} \left(1 + 2\frac{\sin^2 f}{r^2} \right) dS \\ &\sim -\frac{8\pi i C}{3}\tau_i, \end{aligned} \tag{9.44}$$

where the final line is obtained by making use of the asymptotic expression $f(\rho) \sim C/\rho^2$ and keeping only leading order terms in ρ. Next, we have that

$$\begin{aligned}\int_I l_i^{(1)}\, d^3x &= iC\int_I \partial_i\Big(\frac{\mathbf{x}\cdot\boldsymbol{\tau}}{|\mathbf{x}|^3}\Big)\, d^3x = -iC\tau_m \int_I \partial_i\partial_m \frac{1}{|\mathbf{x}|}\, d^3x \\ &= -\frac{iC}{3}\tau_i \int_I \nabla^2 \frac{1}{|\mathbf{x}|}\, d^3x = \frac{4\pi iC}{3}\tau_i\,, \end{aligned} \tag{9.45}$$

where the final expression is obtained by using the identity $\nabla^2 \frac{1}{|\mathbf{x}|} = -4\pi\delta(\mathbf{x})$. Combining these two results we have that

$$\int_I (\tilde{L}_i^{(1)} - l_i^{(1)})\, d^3x \sim -4\pi iC\tau_i\,. \tag{9.46}$$

From (9.38) we see that

$$r_i^{(2)}\Big|_{\mathbf{x}=\mathbf{0}} = iC\mathcal{O}\tau_n\mathcal{O}^\dagger \frac{(\delta_{in} - 3\hat{X}_i\hat{X}_n)}{X^3}\,, \tag{9.47}$$

so the first term in (9.40) has been calculated to be

$$\begin{aligned} -\frac{1}{12\pi^2}\mathrm{Tr}\Big\{ r_i^{(2)}\Big|_{\mathbf{x}=\mathbf{0}} \int_I (\tilde{L}_i^{(1)} &- l_i^{(1)})\, d^3x\Big\} \\ &\sim -\frac{C^2}{3\pi X^3}\mathrm{Tr}(\mathcal{O}\tau_n\mathcal{O}^\dagger\tau_n - 3\hat{X}_i\hat{X}_n\mathcal{O}\tau_n\mathcal{O}^\dagger\tau_i) \\ &= -\frac{2C^2(\mathrm{Tr}M - 3\hat{\mathbf{X}}\cdot M\hat{\mathbf{X}})}{3\pi X^3}\,, \end{aligned} \tag{9.48}$$

where M is the $SO(3)$ matrix corresponding to $\mathcal{O}$ as given in (9.6).

A similar calculation for the second term in (9.40) yields the same result

$$-\frac{1}{12\pi^2}\mathrm{Tr}\Big\{ l_i^{(1)}\Big|_{\mathbf{x}=\mathbf{X}} \int_{II} (\tilde{R}_i^{(2)} - r_i^{(2)})\, d^3x\Big\} \sim -\frac{2C^2(\mathrm{Tr}M - 3\hat{\mathbf{X}}\cdot M\hat{\mathbf{X}})}{3\pi X^3}\,. \tag{9.49}$$

The final term in (9.40) is relatively simple to calculate using an integration by parts and the relation $\nabla^2\frac{1}{|\mathbf{x}|} = -4\pi\delta(\mathbf{x})$.

$$\begin{aligned} -\frac{1}{12\pi^2}\mathrm{Tr}\Big\{ \int_{\mathbb{R}^3} l_i^{(1)} r_i^{(2)}\, d^3x\Big\} &\sim \frac{C^2}{6\pi^2} M_{kj}\int_{\mathbb{R}^3} \partial_i\partial_j \frac{1}{|\mathbf{x}-\mathbf{X}|}\partial_i\partial_k\frac{1}{|\mathbf{x}|}\, d^3x \\ &= \frac{2C^2(\mathrm{Tr}M - 3\hat{\mathbf{X}}\cdot M\hat{\mathbf{X}})}{3\pi X^3}\,. \end{aligned} \tag{9.50}$$

Adding together the three terms in (9.40) we arrive at the final answer

$$E_{\mathrm{int}} \sim -\frac{2C^2(\mathrm{Tr}M - 3\hat{\mathbf{X}}\cdot M\hat{\mathbf{X}})}{3\pi X^3} = \frac{2C^2}{3\pi}(\tilde{\boldsymbol{\partial}}\cdot M\tilde{\boldsymbol{\partial}})\frac{1}{X}\,, \tag{9.51}$$

which agrees with the earlier result obtained from the asymptotic dipole calculation.

The general form of the interaction energy of two charge 1 Skyrmions was originally presented by Skyrme [379] and verified by Jackson *et al.* [218] and Vinh Mau *et al.* [408]. Castillejo and Kugler [76] noted that if the asymptotic interaction energy of two well separated clusters of Skyrmions, of any charge, is positive, then it can be made negative by performing an appropriate isospin transformation on one of the clusters. We have already explicitly seen that this is true in the case of two charge 1 Skyrmions, as illustrated by Eq. (9.31). It may appear that this result constitutes a proof of the strict inequality (9.24), and hence that Skyrmions exist for any baryon number, since it is always possible to arrange that two clusters have a negative interaction energy, and hence a total energy which is lower than the sum of their individual energies. However, the flaw in Castillejo and Kugler's argument is that, to lowest order, the asymptotic interaction energy may vanish. In this case, the lowest order contribution to the asymptotic interaction energy can not be made negative by an isospin rotation and the calculation must be performed to higher order. A similar caveat obviously applies at each order and so it is not possible to conclude that the interaction energy is negative, only that it is non-positive. This is another manifestation of the fact that the weaker energy inequality (9.25) has been proved, but the strict inequality (9.24), required for the proof of existence of arbitrary charge Skyrmions, remains unproven at present.

However, further progress on this problem has recently been made. Now that it has been established that any Skyrmion has a leading multipole [294], it can be shown that in most cases a pair of well separated Skyrmions of any baryon number can be oriented and positioned so as to attract. Unfortunately, the argument breaks down because of the non-linear terms if the leading multipole of one of the Skyrmions is of high order, or more precisely, if the orders of the multipoles differ by more than two. Nevertheless, as Schroers has shown [367], some rigorous conclusions about the existence of Skyrmions of higher baryon number are possible.

9.4 Low charge Skyrmions

In this section we discuss the properties of minimal energy Skyrmions with charges $1 \leq B \leq 8$, constructed using numerical methods. Details of the numerical codes used to compute these solutions can be found in the papers cited below, and a detailed discussion appears in [45], to which we refer the interested reader.

All known solutions appear to be isolated and their only moduli are the obvious ones associated with the nine-dimensional symmetry group of the

Skyrme model. Generic solutions therefore have nine moduli, although solutions with axial or spherical symmetry have, respectively, one or three fewer.

As we have already noted, for charges $B > 1$ the minimal energy Skyrmion is not spherically symmetric. For $B = 2$, it turns out that it has an axial symmetry [244, 283, 406]. The energy density has a similar toroidal structure to that of the charge 2 axisymmetric monopole solution discussed in the previous chapter, despite the fact that the fields of the two models are very different. In displaying Skyrmions it is conventional to plot surfaces of constant baryon density $\mathcal{B}$ (baryon density isosurfaces), where $\mathcal{B}$ is the integrand in Eq. (9.9), although energy density isosurfaces are qualitatively very similar. In Fig. 9.2 we display baryon density isosurfaces for the minimal energy Skyrmions of charges $1 \leq B \leq 8$.

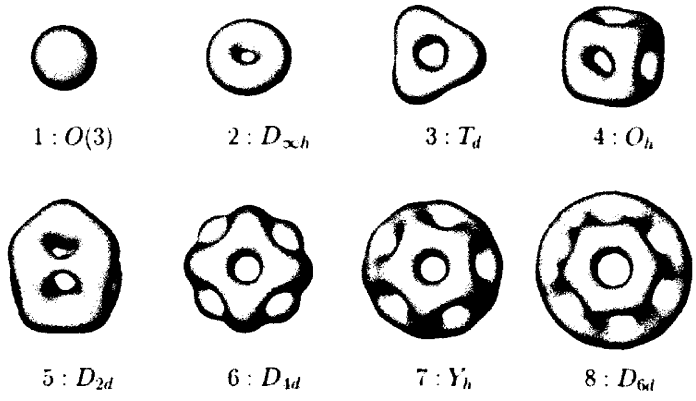

Fig. 9.2. Baryon density isosurfaces for $1 \leq B \leq 8$. The baryon number and symmetry of each solution is shown.

There are axially symmetric solutions of the Skyrme equation for $B > 2$ [244], but these are not the minimal energy solutions, and in fact for $B > 4$ they are not even sufficiently bound to prevent break-up into B single Skyrmions, so they correspond to saddle points.

The Skyrmions presented in Fig. 9.2 have only discrete symmetries for $B > 2$. The $B = 3$ and $B = 4$ Skyrmions have tetrahedral symmetry T_d and cubic symmetry O_h, respectively [65], and again are very similar to particular monopoles of the same charge, which we have already discussed. The associated polyhedra, where the baryon density is concentrated, are a tetrahedron and cube, as the figure shows. It is perhaps of interest to point out that these Skyrmion solutions were computed before the existence of the corresponding monopoles was known. At the time it was therefore very surprising to find these highly symmetric Platonic

Skyrmions emerging from asymmetric initial conditions. Their existence was a major motivation for the search for Platonic monopole solutions, and although a deep connection between Skyrmions and monopoles is still lacking, a link between these two kinds of soliton has been found, via rational maps, and has led to an improved understanding of the structure of Skyrmions, as we discuss in detail in the next section.

The $B = 5$ Skyrmion has a relatively small symmetry, namely D_{2d}. The associated polyhedron comprises four squares and four pentagons, the top and bottom of the structure being related by a relative rotation of 90°. In case the reader is not familiar with extended dihedral symmetries we briefly recount them here. The dihedral group D_n is obtained from C_n, the cyclic group of order n, by the addition of a C_2 axis which is orthogonal to the main C_n symmetry axis. The group D_n can be extended by the addition of a reflection symmetry in two ways: by including a reflection in the plane perpendicular to the main C_n axis, which produces the group D_{nh} or, alternatively, a reflection in a plane which contains the main symmetry axis and bisects a pair of the C_2 axes obtained by applying the C_n symmetry to the generating C_2 axis, which produces the group D_{nd}.

Recall that a charge 5 monopole exists with octahedral symmetry, so given the similarity between monopoles and Skyrmions it may seem a little curious that the $B = 5$ Skyrmion has relatively little symmetry. In fact, as we discuss further in the next section, there is an octahedrally symmetric charge 5 solution, but it is a saddle point whose energy is a little higher than the less symmetric D_{2d} minimum.

The $B = 6$ and $B = 8$ Skyrmions also have extended dihedral symmetries, this time D_{4d} and D_{6d} respectively. The $B = 7$ Skyrmion is icosahedrally symmetric [41], its symmetry group Y_h being an extension of D_{5d}. The baryon density of the $B = 7$ Skyrmion is localized around the edges of a dodecahedron, the structure closely resembling the icosahedrally symmetric charge 7 monopole.

The polyhedron associated with the $B = 6$ Skyrmion consists of two halves, each formed from a square with pentagons hanging down from all four sides. To join these two halves, the two squares must be parallel, with one rotated by 45° relative to the other. The $B = 8$ Skyrmion has a similar structure, except that the squares are replaced by hexagons, and each half has six pentagons hanging down. The top hexagon is parallel to the bottom hexagon but rotated by 30°. The halves of the $B = 7$ Skyrmion have pentagons hanging from a pentagon, hence the larger symmetry.

In Fig. 9.3 we display models (not to scale) of the polyhedra associated with the Skyrmions of charge 5, 6, 7, 8, and in Table 9.1 we present, for charges 1 to 8, the symmetries and energies per baryon, E/B, of the

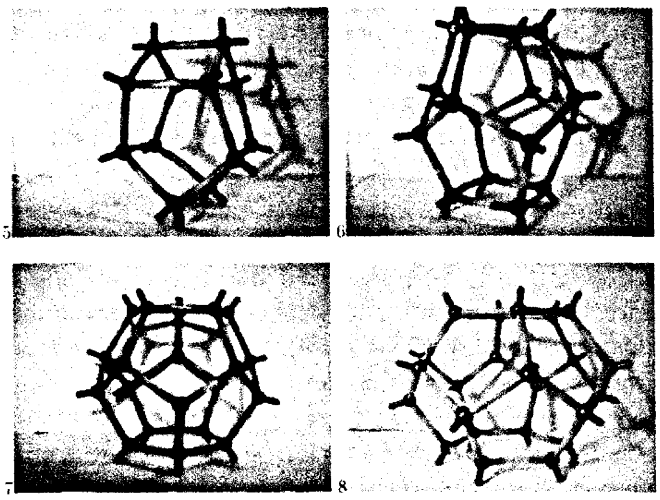

Fig. 9.3. Polyhedral models (not to scale) representing the Skyrmions with $B = 5, 6, 7, 8$.

Skyrmions, computed from the numerical solutions of the field equation [45].

In ref. [41] a phenomenological rule for the structure of the minimal energy Skyrmions was proposed, called the Geometric Energy Minimization (GEM) rule. This states that, for $B > 2$, the polyhedron associated with the charge B Skyrmion is composed of almost regular polygons meeting at $4(B-2)$ trivalent vertices, and the baryon density is concentrated along the edges of the polygons. Note that there are several equivalent ways in which the GEM rule can be stated, since, by using the trivalent property together with Euler's formula, any one of the three parameters of the structure, the number of vertices V, faces F, or edges E, determines the other two. Explicitly, $V = 4(B-2)$, $F = 2(B-1)$, $E = 6(B-2)$. Since the baryon density isosurface has a hole in the centre of each face, the GEM rule is consistent with the observation of ref. [65] that the isosurface contains $2(B-1)$ holes. For $3 \leq B \leq 8$ we have already described the Skyrmions, and it is a simple task to confirm that the GEM rule is obeyed in these cases. However, as B increases, the number of possible structures satisfying the GEM rule grows rapidly, so that by no means does it uniquely predict the structure.

For $B \geq 7$ it is possible to satisfy the GEM rule with a trivalent polyhedron formed from 12 pentagons and $2B-14$ hexagons. We will refer to such structures as fullerene-like and to the conjecture that the Skyrmion's

Table 9.1. The symmetry, K, and energy per baryon, E/B, for the numerically computed minimal energy Skyrmions of charge $1 \leq B \leq 8$.

B	K	E/B
1	$O(3)$	1.2322
2	$D_{\infty h}$	1.1791
3	T_d	1.1462
4	O_h	1.1201
5	D_{2d}	1.1172
6	D_{4d}	1.1079
7	Y_h	1.0947
8	D_{6d}	1.0960

baryon density isosurface has this form as the fullerene hypothesis since precisely the same fullerene (a shortening of Buckminsterfullerene) structures arise in carbon chemistry, where carbon atoms sit at the vertices of such polyhedra [137]. It is then plausible [41] that the minimal energy Skyrmion of charge B has the same symmetry as a fullerene from the family $C_{4(B-2)}$. For low charges ($B = 7$, $B = 8$) this leads to a unique prediction for the structures, which are those we have already encountered, but as the charge increases the number of possible structures again increases. In particular, for $B = 9$ there are two possibilities with D_2 and T_d symmetries respectively, for $B = 10$ there are six, for $B = 11$ there are 15, with a rapid increase for $B > 11$. However, there is a unique icosahedrally symmetric configuration with $B = 17$ corresponding to the famous fullerene structure of C_{60}, and given its high symmetry it is not surprising that the minimal energy $B = 17$ configuration has this structure. In Section 9.6 we discuss Skyrmions of higher charge, up to $B = 22$, and find that the fullerene hypothesis is valid for all but two charges, where interesting caveats apply. In the next section we discuss an approximate analytic description of Skyrmions and see that within this approach at least one aspect of the GEM rule, namely, that the number of faces is $2(B-1)$, can be understood.

9.5 The rational map ansatz

The observed similarities between Skyrmions and monopoles leads naturally to the question whether there is an approximate construction of Skyrmions from monopoles. Of course, it is not expected that an exact correspondence exists, since the Yang-Mills-Higgs and Skyrme models

have a number of very different properties, but for certain monopole solutions a mapping does exist which generates a good approximation to a related exact Skyrmion solution. As yet, there is no known direct transformation between the fields of a monopole and those of a Skyrmion, but as we describe in this section, there is an indirect transformation via rational maps between Riemann spheres. Recall from Chapter 8 that there is a precise correspondence between charge N monopoles and degree N rational maps (we have in mind here the Jarvis maps); thus a Skyrme field constructed from a rational map is indirectly constructed from a monopole.

One needs an ansatz for a Skyrme field in terms of a rational map, and the shell-like fullerene structures of the numerically computed Skyrmions suggest how to proceed. Rational maps are maps from $S^2 \mapsto S^2$, whereas Skyrmions are maps from $\mathbb{R}^3 \mapsto S^3$. The main idea behind the rational map ansatz, introduced in [193], is to identify the domain S^2 of the rational map with concentric spheres in $\mathbb{R}^3$, and the target S^2 with spheres of latitude on S^3. It is convenient to use 3-vector notation to present the ansatz explicitly. Recall that via stereographic projection, the complex coordinate z on a sphere can be identified with conventional polar coordinates by $z = \tan(\theta/2)e^{i\varphi}$. Equivalently, the point z corresponds to the unit vector

$$\hat{\mathbf{n}}_z = \frac{1}{1+|z|^2}(z+\bar{z},\, i(\bar{z}-z),\, 1-|z|^2)\,. \tag{9.52}$$

Similarly the value of the rational map $R(z)$ is associated with the unit vector

$$\hat{\mathbf{n}}_R = \frac{1}{1+|R|^2}(R+\bar{R},\, i(\bar{R}-R),\, 1-|R|^2)\,. \tag{9.53}$$

Let us denote a point in $\mathbb{R}^3$ by its coordinates (r, z), where r is the radial distance from the origin and z specifies the direction from the origin. The ansatz for the Skyrme field, depending on a rational map $R(z)$ and a radial profile function $f(r)$, is

$$U(r,z) = \exp(if(r)\ \hat{\mathbf{n}}_{R(z)} \cdot \boldsymbol{\tau})\,, \tag{9.54}$$

where, as usual, $\boldsymbol{\tau} = (\tau_1, \tau_2, \tau_3)$ denotes the triplet of Pauli matrices. For this to be well defined at the origin, $f(0) = k\pi$ for some integer k. We take $k = 1$ in what follows. The boundary condition $U = 1_2$ at $r = \infty$ is satisfied by setting $f(\infty) = 0$. It is straightforward to verify (see below) that the baryon number of this field configuration is $B = N$, where N is the degree of R.

Mathematically, this construction of a map from compactified $\mathbb{R}^3$ to S^3, out of a map from S^2 to S^2, is a suspension; the suspension points on the domain are the origin and the point at infinity, and on the target the

points $U = -1_2$ and $U = 1_2$. Suspension is an isomorphism between the homotopy groups $\pi_2(S^2)$ and $\pi_3(S^3)$, which explains why $B = N$.

An $SU(2)$ Möbius transformation on the domain S^2 of the rational map corresponds to a spatial rotation, whereas an $SU(2)$ Möbius transformation on the target S^2 corresponds to a rotation of $\hat{\mathbf{n}}_R$, and hence to an isospin rotation of the Skyrme field. Thus if a rational map $R : S^2 \mapsto S^2$ is symmetric in the sense defined in Chapter 6 (i.e. a rotation of the domain can be compensated by a rotation of the target), then the resulting Skyrme field is symmetric in the sense defined in Section 9.2 (i.e. a spatial rotation can be compensated by an isospin rotation).

Note that if we introduce the Hermitian projector

$$P = \frac{1}{1+|R|^2}\begin{pmatrix} 1 & \bar{R} \\ R & |R|^2 \end{pmatrix}, \tag{9.55}$$

satisfying $P^2 = P = P^\dagger$, then the ansatz (9.54) can be written as

$$U = \exp(if(2P - 1_2)). \tag{9.56}$$

which is similar to the expression (8.262), describing the asymptotic form of the solution of the Jarvis equation corresponding to the monopole with rational map R.

The simplest degree 1 rational map is $R = z$, which is spherically symmetric. The ansatz (9.54) then reduces to Skyrme's hedgehog field (9.18) with $f(r)$ being the usual profile function. In this case the ansatz is compatible with the static Skyrme equation but in general it is not, so it can not produce exact solutions, only low energy approximations to these.

An attractive feature of the ansatz is that it leads to a simple energy expression which can be minimized with respect to the rational map R and the profile function f to obtain close approximations to the numerical, exact Skyrmion solutions. To calculate the energy we exploit the geometrical formulation of the Skyrme model presented in Section 9.1. For the ansatz (9.54), the strain in the radial direction is orthogonal to the strain in the angular directions. Moreover, because $R(z)$ is conformal, the angular strains are isotropic. If we identify λ_1^2 with the radial strain and λ_2^2 and λ_3^2 with the angular strains, we can easily compute that

$$\lambda_1 = -f'(r), \quad \lambda_2 = \lambda_3 = \frac{\sin f}{r}\frac{1+|z|^2}{1+|R|^2}\left|\frac{dR}{dz}\right|. \tag{9.57}$$

From Eq. (9.12), the baryon number is

$$B = -\int \frac{f'}{2\pi^2}\left(\frac{\sin f}{r}\frac{1+|z|^2}{1+|R|^2}\left|\frac{dR}{dz}\right|\right)^2 \frac{2i\,dz d\bar{z}}{(1+|z|^2)^2}\, r^2\, dr, \tag{9.58}$$

where $2i\,dzd\bar{z}/(1+|z|^2)^2$ is equivalent to the usual area element on a 2-sphere $\sin\theta\,d\theta d\varphi$. Now the part of the integrand

$$\left(\frac{1+|z|^2}{1+|R|^2}\left|\frac{dR}{dz}\right|\right)^2 \frac{2i\,dzd\bar{z}}{(1+|z|^2)^2} \tag{9.59}$$

is precisely the pull-back of the area form $2i\,dRd\bar{R}/(1+|R|^2)^2$ on the target sphere of the rational map R; therefore its integral is 4π times the degree N of R. So (9.58) simplifies to

$$B = -\frac{2N}{\pi}\int_0^\infty f'\sin^2 f\,dr = N\,, \tag{9.60}$$

where we have used the boundary conditions $f(0)=\pi$, $f(\infty)=0$. This verifies again that the baryon number of the Skyrme field generated from the ansatz is equal to the degree of the rational map.

Substituting the strains (9.57) into the expression (9.12) for the energy density yields the energy

$$\begin{aligned} E = \frac{1}{12\pi^2}\int\Bigg\{ & f'^2 + 2\frac{\sin^2 f}{r^2}(f'^2+1)\left(\frac{1+|z|^2}{1+|R|^2}\left|\frac{dR}{dz}\right|\right)^2 \\ & + \frac{\sin^4 f}{r^4}\left(\frac{1+|z|^2}{1+|R|^2}\left|\frac{dR}{dz}\right|\right)^4\Bigg\}\frac{2i\,dzd\bar{z}}{(1+|z|^2)^2}\,r^2\,dr\,, \end{aligned} \tag{9.61}$$

which can be simplified, using the above remarks about baryon number, to

$$E = \frac{1}{3\pi}\int_0^\infty \left(r^2 f'^2 + 2B\sin^2 f(f'^2+1) + \mathcal{I}\frac{\sin^4 f}{r^2}\right)dr\,. \tag{9.62}$$

$\mathcal{I}$ denotes the purely angular integral

$$\mathcal{I} = \frac{1}{4\pi}\int\left(\frac{1+|z|^2}{1+|R|^2}\left|\frac{dR}{dz}\right|\right)^4 \frac{2i\,dzd\bar{z}}{(1+|z|^2)^2}\,, \tag{9.63}$$

which only depends on the rational map R.

Note the following pair of inequalities associated with the expression (9.62) for the energy E. The elementary inequality

$$\left(\int 1\,dS\right)\left(\int\left(\frac{1+|z|^2}{1+|R|^2}\left|\frac{dR}{dz}\right|\right)^4 dS\right) \geq \left(\int\left(\frac{1+|z|^2}{1+|R|^2}\left|\frac{dR}{dz}\right|\right)^2 dS\right)^2. \tag{9.64}$$

where $dS = 2i\,dzd\bar{z}/(1+|z|^2)^2$, implies that $\mathcal{I}\geq B^2$. Next, by using a Bogomolny-type argument, we see that

$$\begin{aligned} E = \frac{1}{3\pi}\int_0^\infty\Bigg\{ & \left(rf' + \sqrt{\mathcal{I}}\,\frac{\sin^2 f}{r}\right)^2 + 2B\sin^2 f(f'+1)^2 \\ & - 2(2B+\sqrt{\mathcal{I}})f'\sin^2 f\Bigg\}\,dr \end{aligned} \tag{9.65}$$

so

$$E \geq \frac{1}{3\pi}(2B+\sqrt{\mathcal{I}})\int_0^\infty (-2f'\sin^2 f)\,dr = \frac{1}{3\pi}(2B+\sqrt{\mathcal{I}})\Big[-f+\frac{1}{2}\sin 2f\Big]_0^\infty \tag{9.66}$$

and so

$$E \geq \frac{1}{3}(2B+\sqrt{\mathcal{I}})\,. \tag{9.67}$$

Combined with the earlier inequality for $\mathcal{I}$, we recover the usual Fadeev-Bogomolny bound $E \geq B$. The bound (9.67) is stronger than this for fields given by the rational map ansatz, but there is no reason to think that true solutions of the Skyrme equation are constrained by this bound.

To minimize E one should first minimize $\mathcal{I}$ over all maps of degree B. The profile function f minimizing the energy (9.62) may then be found by a simple gradient flow algorithm with B and $\mathcal{I}$ as fixed parameters. In Section 9.6 we discuss the results of a numerical search for $\mathcal{I}$-minimizing maps among all rational maps of degree B, but in this section we first consider the simpler problem in which we restrict the map to a given symmetric form, with symmetries corresponding to one of the numerically known Skyrmion solutions. If these maps still contain a few free parameters, $\mathcal{I}$ can be minimized with respect to these. This procedure is appropriate for all baryon numbers up to $B = 8$, for which we know the symmetries of the numerically computed Skyrmions, and there is sufficient symmetry to highly constrain the rational map.

For $B = 2, 3, 4, 7$ the symmetries of the numerically computed Skyrmions are $D_{\infty h}, T_d, O_h, Y_h$ respectively. From the general discussion and specific examples of Chapters 6 and 8, we see that in each of these cases there is a unique rational map with the given symmetry. We recall that they are

$$R = z^2,\ R = \frac{z^3-\sqrt{3}iz}{\sqrt{3}iz^2-1},\ R = \frac{z^4+2\sqrt{3}iz^2+1}{z^4-2\sqrt{3}iz^2+1},\ R = \frac{z^7-7z^5-7z^2-1}{z^7+7z^5-7z^2+1}. \tag{9.68}$$

Using these maps, and computing the optimal profile functions $f(r)$, one obtains Skyrme fields whose baryon density isosurfaces are indistinguishable from those presented in Fig. 9.2. In Table 9.2 we list the energies per baryon of the approximate solutions obtained using the rational map ansatz, together with the values of $\mathcal{I}$ and $\mathcal{I}/B^2$, in order to compare with the bound $\mathcal{I}/B^2 \geq 1$.

Recall that the Wronskian of a rational map $R(z) = p(z)/q(z)$ of degree B is the polynomial

$$W(z) = p'(z)q(z) - q'(z)p(z) \tag{9.69}$$

of degree $2B-2$, and observe that the zeros of the Wronskian give interesting information about the shape of the Skyrme field constructed using

Table 9.2. Approximate Skyrmions obtained using the rational map ansatz. For $1 \leq B \leq 8$ we list the symmetry of the rational map, K, the value of $\mathcal{I}$, its comparison with the bound $\mathcal{I}/B^2 \geq 1$, and the energy per baryon E/B obtained after computing the profile function which minimizes the Skyrme energy function.

B	K	$\mathcal{I}$	$\mathcal{I}/B^2$	E/B
1	$O(3)$	1.0	1.000	1.232
2	$D_{\infty h}$	5.8	1.452	1.208
3	T_d	13.6	1.509	1.184
4	O_h	20.7	1.291	1.137
5	D_{2d}	35.8	1.430	1.147
6	D_{4d}	50.8	1.410	1.137
7	Y_h	60.9	1.242	1.107
8	D_{6d}	85.6	1.338	1.118

the ansatz (9.54). Where W is zero, the derivative dR/dz is zero, so the strain eigenvalues in the angular directions, λ_2 and λ_3, vanish. The baryon density, being proportional to $\lambda_1\lambda_2\lambda_3$, therefore vanishes along the entire radial line in the direction specified by any zero of W. The energy density will also be low along such a radial line, since there will only be the contribution λ_1^2 from the radial strain eigenvalue. The ansatz thus makes manifest why the Skyrme field baryon density contours look like polyhedra with holes in the directions given by the zeros of W, and why there are $2B-2$ such holes, precisely the structure seen in all the plots in Fig. 9.2. This explains the GEM rule $F = 2(B-1)$, and although there is no firm rational map explanation of the other aspects of the GEM rule, we will make some further comments on them in the following section.

As an example, consider the icosahedrally symmetric degree 7 map in (9.68). The Wronskian is

$$W(z) = 28z(z^{10} + 11z^5 - 1), \tag{9.70}$$

which is proportional to the Klein polynomial $\mathcal{Y}_v$, and it vanishes at the twelve face centres of a dodecahedron [237]. This explains why the baryon density isosurface of the $B = 7$ Skyrmion displayed in Fig. 9.2 is localized around the edges of a dodecahedron.

For the remaining charges, $B = 5, 6, 8$, the Skyrmions have extended dihedral symmetries, so we need to consider degree B rational maps with dihedral symmetries D_n, and their extensions by reflections to D_{nd} and D_{nh}. Constructing D_n-symmetric maps does not require the general group

theory formalism discussed in Chapter 6 since it is simple to explicitly apply the two generators of D_n to a map. In terms of the Riemann sphere coordinate z the generators of the dihedral group D_n may be taken to be $z \mapsto e^{2\pi i/n} z$ and $z \mapsto 1/z$. The reflection required to extend the symmetry to D_{nh} is represented by $z \mapsto 1/\bar{z}$, whereas $z \mapsto e^{\pi i/n}\bar{z}$ results in the symmetry group D_{nd}.

Explicitly, an s-parameter family of D_n-symmetric maps is given by*

$$R(z) = \frac{\sum_{j=0}^{s} a_j z^{jn+u}}{\sum_{j=0}^{s} a_{s-j} z^{jn}}, \tag{9.71}$$

where $u = B \bmod n$ and $s = (B-u)/n$. Here $a_s = 1$ and $a_0, \ldots, a_{s-1}$ are arbitrary complex parameters. Clearly, these maps satisfy the conditions for symmetry under D_n,

$$R(e^{2\pi i/n} z) = e^{2\pi i u/n} R(z), \quad R(1/z) = 1/R(z), \tag{9.72}$$

and imposing a reflection symmetry constrains each complex coefficient a_j to be either real, or pure imaginary. In the case of D_{nh} symmetry, all coefficients a_j are real, whereas for D_{nd} symmetry a_j is real or imaginary depending on whether $(s-j) \bmod 2$ is, respectively, 0 or 1.

Consider now the $B = 5$ maps with D_{2d} symmetry. Setting $B = 5$ and $n = 2$ in the above gives $u = 1$ and $s = 2$, so there is a family of degree 5 maps with two real parameters,

$$R(z) = \frac{z(a + ibz^2 + z^4)}{1 + ibz^2 + az^4}, \tag{9.73}$$

with a and b real. Additional symmetry occurs if $b = 0$; $R(z)$ then has D_{4h} symmetry, the symmetry of a square. There is octahedral symmetry if, in addition, $a = -5$. This value ensures the 120° rotational symmetry

$$R\left(\frac{iz+1}{-iz+1}\right) = \frac{iR(z)+1}{-iR(z)+1}. \tag{9.74}$$

The octahedral map $R(z) = z(z^4 - 5)/(-5z^4 + 1)$ has Wronskian

$$W(z) = -5(z^8 + 14z^4 + 1), \tag{9.75}$$

which is proportional to $\mathcal{O}_f$, the face polynomial of an octahedron. Using (9.73) in the rational map ansatz for the Skyrme field gives a structure which is a polyhedron with eight faces. In the special case $a = -5$, $b = 0$, this polyhedron is an octahedron, and the angular integral is $\mathcal{I} = 52.1$; however, a numerical search over the parameters a and b shows that $\mathcal{I}$

* There are other D_n-symmetric families of maps, but we will not need these.

is minimized when $a = -3.07$, $b = 3.94$, taking the value $\mathcal{I} = 35.8$. The approximate Skyrmion generated from the map with these parameter values has a baryon density isosurface which is virtually identical to that of the numerically computed solution displayed in Fig. 9.2. From this analysis we therefore understand that there is an octahedrally symmetric $B = 5$ solution, but that it is a saddle point with an energy higher than that of the less symmetric D_{2d} Skyrmion. There is a further, higher saddle point at $a = b = 0$, where the map (9.73) simplifies to $R(z) = z^5$, and gives a toroidal Skyrme field. Although many minimal energy Skyrmions are highly symmetric, symmetry is not the most important factor in determining the structure of the minimal energy solution, and less symmetric configurations sometimes have lowest energy.

Another example of a symmetric saddle point is the $B = 7$ configuration with cubic symmetry. The relevant rational map is given by $R(z) = (7z^4 + 1)/(z^7 + 7z^3)$ and has Wronskian $W(z) = -21z^2(z^4 - 1)^2$. Each root of this Wronskian is a double root (including the one at infinity) and they lie at the face centres of a cube. A baryon density isosurface for this saddle point configuration is therefore qualitatively similar to that of the minimal energy $B = 4$ Skyrmion. This cubic $B = 7$ saddle point will play a role in a scattering process discussed in Chapter 10.

The analysis of the relevant dihedrally symmetric $B = 6$ and $B = 8$ maps is similar to the $B = 5$ case, the only difference being that just one real parameter appears, so the energy minimization is easier. These maps can be found in ref. [193].

Given the rational map describing a Skyrmion it is possible to infer information regarding its asymptotic fields. For a Skyrmion which is symmetric under a group K, its pion fields will be invariant under combinations of rotations by elements of K and isospin rotations given by some (not necessarily irreducible) real three-dimensional representation of K, which we denote by ρ. Now the dipole fields of a single Skyrmion, being spherically symmetric, are also K-symmetric by restriction, and the corresponding representation ρ is the defining representation of K, regarded as a subgroup of $SO(3)$, which we denote by $\hat{\rho}$, so $\hat{\rho}(k) = k$. By comparing ρ and $\hat{\rho}$ it is possible to determine whether a given Skyrmion looks from far away like a single Skyrmion or antiSkyrmion, that is, like a triplet of orthogonal dipoles. This information is important in understanding the interaction between Skyrmion solutions and will be used in Section 9.8 when we discuss Skyrmion dynamics and scattering.

As an example, consider the tetrahedrally symmetric $B = 3$ Skyrmion described by the map $R(z) = (z^3 - \sqrt{3}iz)/(\sqrt{3}iz^2 - 1)$. A straightforward calculation reveals that $\rho = \hat{\rho} = F$, that is, the pion fields transform via the same three-dimensional irreducible representation of the tetrahedral group as the hedgehog fields of a single Skyrmion or antiSkyrmion. In

order to distinguish between these last two possibilities we can compute the value of the rational map along the three Cartesian directions, finding $R(0) = 0$, $R(1) = -1$, $R(i) = i$, which demonstrates that the asymptotic dipole fields are those of an antiSkyrmion, since the pion fields are obtained from those of a Skyrmion by the reflection $\pi_2 \mapsto -\pi_2$.

The fact that the $B = 3$ Skyrmion is asymptotically like an anti-Skyrmion can be understood more naively by a simple addition of the dipole moments of its constitutent single Skyrmions. First consider two single Skyrmions brought together along the x^1-axis. They are in the attractive channel if the first is in standard orientation and the second is rotated by 180° around the x^3-axis. This gives triplets of dipole moments $\mathbf{p} = 4\pi C(\mathbf{e}_1, \mathbf{e}_2, \mathbf{e}_3)$ and $\mathbf{q} = 4\pi C(-\mathbf{e}_1, -\mathbf{e}_2, \mathbf{e}_3)$. Their sum is $4\pi C(\mathbf{0}, \mathbf{0}, 2\mathbf{e}_3)$, implying that the toroidal $B = 2$ Skyrmion has only a single dipole, with roughly twice the usual strength. Now bring in a third Skyrmion, along the x^3-axis, and rotated by 180° around the x^1-axis, giving the dipole moments $\mathbf{r} = 4\pi C(\mathbf{e}_1, -\mathbf{e}_2, -\mathbf{e}_3)$. The total of the dipoles is $\mathbf{p} + \mathbf{q} + \mathbf{r} = 4\pi C(\mathbf{e}_1, -\mathbf{e}_2, \mathbf{e}_3)$, precisely those of an antiSkyrmion.

A similar analysis suggests that the $B = 4$ cubic Skyrmion will have no dipoles, since it can be constructed from two $B = 2$ tori. These have a single dipole each, which by an appropriate relative isospin rotation can be made to cancel. The symmetry of the degree 4 cubic map (9.68) is consistent with this result, since the representation ρ is the sum of a one- and two-dimensional irreducible representation of O, whereas $\hat{\rho}$ is a three-dimensional irreducible representation. The fact that the $B = 4$ Skyrmion has no dipole fields explains why it is so tightly bound, and why it interacts only weakly with other Skyrmions.

For the dodecahedral $B = 7$ Skyrmion the naive dipole picture appears to fail, since the combination of the $B = 4$ cubic Skyrmion, with no dipole fields, and the $B = 3$ tetrahedral Skyrmion, with antiSkyrmion dipole fields, suggests that the $B = 7$ Skyrmion has the dipole fields of an antiSkyrmion. However, the representation analysis of the degree 7 dodecahedral map (9.68) reveals that although both ρ and $\hat{\rho}$ are three-dimensional irreducible representations of Y, they are not the same (one is F_1 and the other is F_2). Hence the asymptotic fields can not be those of a single antiSkyrmion (or Skyrmion). In fact, there are no dipole moments at all. The reason why the simple dipole picture fails in this case is not yet understood.

9.6 Higher charge Skyrmions

In the preceding section, for each charge $B \leq 8$, the map R was selected so that the symmetry of the resulting Skyrme field matched that of the numerically computed Skyrmion. Recently, an alternative approach to

Table 9.3. Results from the simulated annealing of rational maps of degree B. For $9 \leq B \leq 22$ we list the symmetry of the rational map, K, the minimal value of $\mathcal{I}$, the value of $\mathcal{I}/B^2$ (which is bounded below by 1), and the energy per baryon E/B obtained after computing the profile function which minimizes the Skyrme energy functional.

B	K	$\mathcal{I}$	$\mathcal{I}/B^2$	E/B
9	D_{4d}	109.3	1.349	1.116
10	D_{4d}	132.6	1.326	1.110
11	D_{3h}	161.1	1.331	1.109
12	T_d	186.6	1.296	1.102
13	O	216.7	1.282	1.098
14	D_2	258.5	1.319	1.103
15	T	296.3	1.317	1.103
16	D_3	332.9	1.300	1.098
17	Y_h	363.4	1.257	1.092
18	D_2	418.7	1.292	1.095
19	D_3	467.9	1.296	1.095
20	D_{6d}	519.7	1.299	1.095
21	T	569.9	1.292	1.094
22	D_{5d}	621.6	1.284	1.092

constructing the appropriate rational map R, based on energy minimization rather than symmetry, has been applied for all charges $B \leq 22$ [45]. In this approach, no assumption is made as to the possible symmetry of the minimal energy Skyrmion, which has the advantage that full numerical simulations of the Skyrme equation need not first be performed (although it is obviously useful to have these results for comparison, as we discuss later). The main task is to search for the rational map of degree B that minimizes $\mathcal{I}$, which may be viewed as an interesting energy function on the space of rational maps. This is still quite difficult numerically but has been performed using a simulated annealing algorithm, a Monte-Carlo based minimization method which has a major advantage over other conventional minimization techniques in that changes which increase the energy are allowed, enabling the algorithm to escape from local minima that are not the global minimum.

For $B \leq 8$ the simulated annealing algorithm reproduces the rational maps discussed previously (whose properties are listed in Table 9.2), providing a nice numerical check on both the minimizing rational map

strategy and also the full field simulations – since these produce very similar configurations.

The results of the simulated annealing algorithm applied to a general rational map of degree $9 \leq B \leq 22$ are presented in Table 9.3. In each case, we tabulate the identified symmetry group K, the minimum value of $\mathcal{I}$, the quantity $\mathcal{I}/B^2$ (which is strikingly uniform at around 1.25–1.35), and the value of E/B for the profile function which minimizes the energy functional (9.62) for the particular map.

By minimizing within certain symmetric families of maps, where the symmetries are *not* shared by the minimal energy map, it is possible to find other critical points of $\mathcal{I}$. In Table 9.4 we present the results of an extensive search for such minimal energy maps with particular symmetries, usually dihedral groups or those groups suggested by the extensive tables of fullerenes presented in ref. [137], which lends further weight to the conclusion that the maps presented in Table 9.3 are in fact the global minima for the energy functional $\mathcal{I}$. These results do, however, turn up the possibility that in certain cases the $\mathcal{I}$-minimizing map may not necessarily be the one which represents the true Skyrmion, since some of the $\mathcal{I}$ values in Tables 9.4 and 9.3 are very close. For the moment we will denote the maps in Table 9.4 by $*$, and conclude at least that they are not global minima of $\mathcal{I}$, but represent other critical points.

For most charges there is a sufficient gap between the minimal value of $\mathcal{I}$ and that of any other critical point to be confident that the minimal map corresponds to the Skyrmion. However, for charges $B = 10, 16, 22$ a glance at Tables 9.3 and 9.4 reveals that there are different maps (with different symmetries) whose associated Skyrme fields have energies which differ by less than 0.1%. Given that the rational map ansatz is an approximation which tends to overestimate the energy by around 1%, it is not clear which of these maps will best describe the angular form of the minimal energy Skyrmion. This question has been addressed using full field simulations [45] in which various initial conditions, consisting of a number of well separated Skyrmion clusters, are relaxed. Although it is difficult to make definitive statements, the results suggest that for these three charges the maps presented in Table 9.4, rather than in Table 9.3, represent the minimal energy Skyrmions. The case $B = 14$ is anomalous, in that the rational map describing the Skyrmion, which again is not the $\mathcal{I}$-minimizing map, is not currently known. The solution obtained from full field simulations (believed to be the minimal energy configuration) is rather elongated, so the rational map approximation to this configuration probably has a substantially higher energy, since it assumes a spherical shape. This explains why it is likely that the rational map which describes the more spherical version of this Skyrmion is not the $\mathcal{I}$-minimizing map. There is a technical reason why we are unable to compute this map,

Table 9.4. Same as for Table 9.3, but for other critical points of $\mathcal{I}$. Notice that the $\mathcal{I}$ values for the $B = 10$ configurations with D_3 and D_{3d} symmetry, for $B = 13$ with D_{4d}, $B = 16$ with D_2, and $B = 22$ with D_3 are extremely close to the corresponding values in Table 9.3, suggesting the possibility of local minima or low-lying saddle points.

B	K	$\mathcal{I}$	$\mathcal{I}/B^2$	E/B
9*	T_d	112.8	1.393	1.123
10*	D_3	132.8	1.328	1.110
10*	D_{3d}	133.5	1.335	1.111
10*	D_{3h}	143.2	1.432	1.126
13*	D_{4d}	216.8	1.283	1.098
13*	O_h	265.1	1.568	1.140
15*	T_d	313.7	1.394	1.113
16*	D_2	333.4	1.302	1.098
17*	O_h	367.2	1.271	1.093
19*	T_h	469.8	1.301	1.096
22*	D_3	623.4	1.288	1.092

which is that the associated Skyrmion has very little symmetry, in fact only C_2, and this is already contained within the symmetry group of the $\mathcal{I}$-minimizing map, which is D_2.

Taking into account the above comments, we present, in Table 9.5, the symmetry K, and energy per baryon E/B, for all minimal energy Skyrmions with $B \leq 22$. These values were computed by relaxation of the full Skyrme energy function with initial conditions created from the corresponding rational map (see ref. [45] for further details). We also list the energy E, the ionization energy $I = E_{B-1} + E_1 - E_B$, which is the energy required to remove a single Skyrmion, and the binding energy per baryon given by $\Delta E/B = E_1 - (E/B)$, which is the energy required to separate the solution into single Skyrmions divided by the total baryon number.

In Fig. 9.4 we plot baryon density isosurfaces (to scale) for each of the Skyrmions with $7 \leq B \leq 22$, and also display models (not to scale) of the associated polyhedra. For all charges except $B = 9$ and $B = 13$ (which we discuss below) the Skyrmions are fullerene-like, and the associated polyhedra can be found in the classification of fullerenes [137].

A particularly interesting example is the $B = 17$ Skyrmion, which has the icosahedrally symmetric structure of the famous C_{60} Buckyball, as

Table 9.5. A summary of the symmetries and energies of the Skyrmion configurations which have been identified as the energy minima. Included also are the ionization energy I – that required to remove one Skyrmion – and the binding energy per Skyrmion $\Delta E/B$ – the energy required to split the charge B Skyrmion into B charge 1 Skyrmions divided by the total number of Skyrmions. (*) This symbol indicates Skyrmions whose angular form differs from that of the minimal energy solutions within the rational map ansatz. (**) The values quoted for $B = 14$ are computed using an initial configuration with D_2 symmetry.

B	K	E/B	E	I	$\Delta E/B$
1	$O(3)$	1.2322	1.2322	0.0000	0.0000
2	$D_{\infty h}$	1.1791	2.3582	0.1062	0.0531
3	T_d	1.1462	3.4386	0.1518	0.0860
4	O_h	1.1201	4.4804	0.1904	0.1121
5	D_{2d}	1.1172	5.5860	0.1266	0.1150
6	D_{4d}	1.1079	6.6474	0.1708	0.1243
7	Y_h	1.0947	7.6629	0.2167	0.1375
8	D_{6d}	1.0960	8.7680	0.1271	0.1362
9	D_{4d}	1.0936	9.8424	0.1578	0.1386
10*	D_3	1.0904	10.9040	0.1706	0.1418
11	D_{3h}	1.0889	11.9779	0.1583	0.1433
12	T_d	1.0856	13.0272	0.1829	0.1466
13	O	1.0834	14.0842	0.1752	0.1488
14**	C_2	1.0842	15.1788	0.1376	0.1480
15	T	1.0825	16.2375	0.1735	0.1497
16*	D_2	1.0809	17.2944	0.1753	0.1513
17	Y_h	1.0774	18.3158	0.2108	0.1548
18	D_2	1.0788	19.4184	0.1296	0.1534
19	D_3	1.0786	20.4934	0.1572	0.1536
20	D_{6d}	1.0779	21.5580	0.1676	0.1543
21	T_d	1.0780	22.6380	0.1522	0.1542
22*	D_3	1.0766	23.6852	0.1850	0.1556

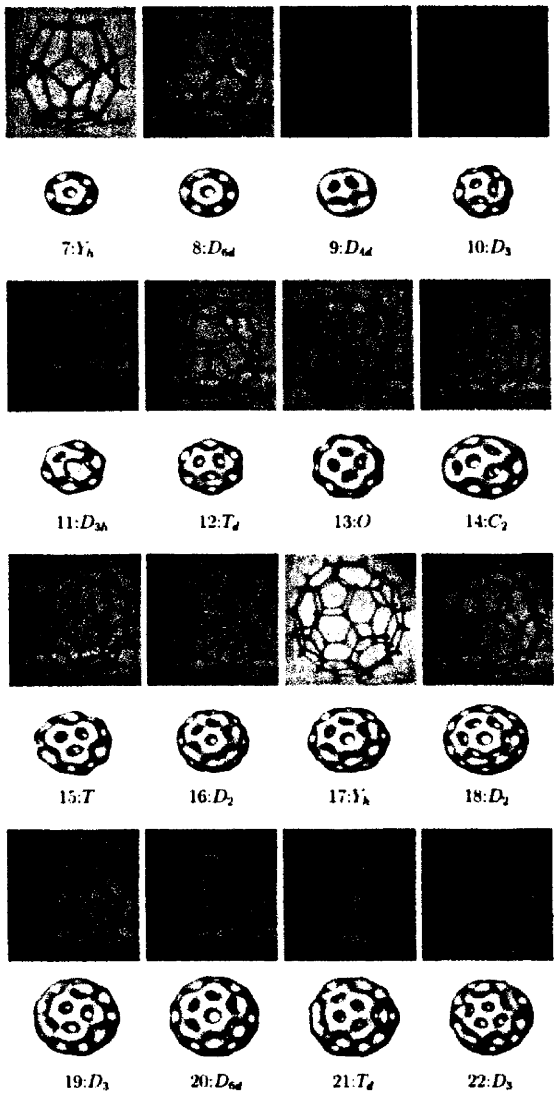

Fig. 9.4. Baryon density isosurfaces for $7 \leq B \leq 22$, and the associated symmetry groups and polyhedral models (not to scale).

indicated earlier. It is formed from 12 pentagons and 20 hexagons and is the structure with isolated pentagons having the least number of vertices. The decomposition which determines the relevant rational map is

$$\underline{18}|_Y = E_2' \oplus G' \oplus 2I', \tag{9.76}$$

whose single two-dimensional component E_2' demonstrates that there is a unique Y-symmetric degree 17 map. In fact, the map is [193]

$$R(z) = \frac{17z^{15} - 187z^{10} + 119z^5 - 1}{z^2(z^{15} + 119z^{10} + 187z^5 + 17)}, \tag{9.77}$$

and it is Y_h-symmetric.

In general, even in highly symmetric cases there will still be a few parameters in the family of symmetric maps of interest. For example, the decomposition

$$\underline{6n+4}|_T = nE' \oplus (n \oplus 1)E_1' \oplus (n \oplus 1)E_2', \tag{9.78}$$

valid for any non-negative integer n, shows that there is an n-parameter family of tetrahedral maps of degree $B = 6n + 3$, corresponding to the middle component in the above. For $n = 0, 2, 3$ ($B = 3, 15, 21$) this family includes the minimal energy map, and for $n = 1$ ($B = 9$) it includes a map which is very close to minimal. Thus it seems possible that other members of this family will be minimal maps, for example, for $B = 27$. The explicit form of all the relevant rational maps for $B \leq 22$ can be found in ref. [45].

The charge $B = 9$ and $B = 13$ Skyrmions are not fullerene-like. Their symmetry groups, D_{4d} and O, both contain C_4 subgroups, and this is incompatible with the trivalent vertex structure of a fullerene. As can clearly be seen in Fig. 9.4, these Skyrmions both contain tetravalent vertices, which can be obtained from fullerenes by a process known as symmetry enhancement (see Fig. 9.5).

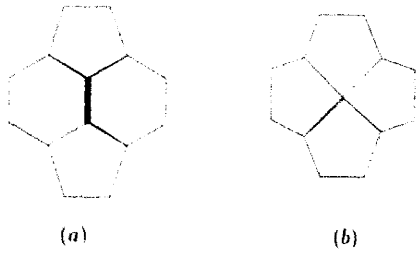

Fig. 9.5. An illustration of symmetry enhancement.

Consider part of a fullerene with the form shown in Fig. 9.5(a), consisting of two pentagons and two hexagons with a C_2 symmetry. The symmetry enhancement process shrinks the edge common to the two hexagons (the thick line) to zero length, resulting in the coalescence of two vertices. The object formed is shown in Fig. 9.5(b). It has a tetravalent vertex connecting four pentagons and the symmetry is enhanced to C_4. We find, empirically, that pairs of symmetry enhancement processes occur on antipodal edges of a fullerene structure.

There is a C_{28} fullerene with D_2 symmetry (denoted 28:1 in ref. [137]) that contains two of the structures shown in Fig. 9.5(a). If symmetry enhancement is performed on both, then the resulting object is precisely the D_{4d} configuration of the $B = 9$ Skyrmion described earlier. There are also D_2-symmetric C_{44} fullerenes (denoted 44:75 and 44:89 in ref. [137]) with an equal number of pentagons and hexagons (12 of each), and a very symmetric configuration can be obtained by symmetry enhancement at all six possible vertices, which results in the cubic $B = 13$ Skyrmion.

In the context of fullerenes it is, of course, impossible for vertices to coalesce since they correspond to the positions of the carbon atoms, but for Skyrmions the vertices represent concentrations of the baryon density and they need not be distinct; it just appears that in most cases it is energetically favourable to have distinct vertices. Note that, by an examination of the baryon density isosurface by eye, it can often be difficult to identify whether a given vertex is trivalent or tetravalent, since the edge length which must be zero for symmetry enhancement could be small, but non-zero.

Although we do not have a general global characterization of the vertices of the polyhedron associated with a rational map (as we do for the face centres, via the Wronskian) it is possible, by a local analysis of the rational map, to check whether a given point is a local baryon density maximum and to obtain its valency. By using the freedom to perform rotations of both the domain and target 2-spheres it is always possible to choose the given point to be $z = 0$ and the rational map to have a local expansion

$$R(z) = \alpha(z + \beta z^{p+1} + O(z^{p+2})), \tag{9.79}$$

where α and β are real positive constants. (The derivative of the map is non-zero at $z = 0$, since the baryon density is assumed to be non-zero there.)

Substituting the expansion (9.79) into the expression for the angular contribution to the baryon density (9.59) we obtain the following result. If $p = 1$ then $z = 0$ is not a vertex. If $p > 2$ and $\alpha > 1$ then $z = 0$ is a p-valent vertex, with the baryon density being a local maximum there. The remaining case of $p = 2$ is a little more subtle. In many cases,

all the local maxima of the baryon density correspond to vertices of the polyhedron. However, in some cases (the lowest charge example being $B = 5$) some of the maxima are at edge midpoints. Such edges may consequently appear thicker than others. The rational map description of such a bivalent maximum is the $p = 2$ case, and a local maximum requires that $\alpha > \sqrt{1+3\beta}$.

To illustrate this analysis, consider the cubic $B = 13$ Skyrmion. For computing O-symmetric degree 13 maps the relevant decomposition is

$$\underline{14}|_O = 2E_2' \oplus E_1' \oplus 2G' . \tag{9.80}$$

From the $2E_2'$ component there is a 1-parameter family of maps, with the explicit form

$$R(z) = \frac{z(a + (6a - 39)z^4 - (7a + 26)z^8 + z^{12})}{1 - (7a + 26)z^4 + (6a - 39)z^8 + az^{12}} , \tag{9.81}$$

whose minimal value of $\mathcal{I}$ occurs at $a = 0.40 + 5.18i$. This gives a Skyrme field whose baryon density is virtually identical to the one shown in Fig. 9.4. The associated polyhedron is similar to a cube, each face of which consists of four pentagons with a tetravalent bond. In order for them to fit together, with all the other bonds being trivalent, each of the six faces must be rotated slightly relative to the one diametrically opposite, which removes the possibility of the cube having reflection symmetries and symmetry group O_h. The polyhedron has 24 pentagonal faces, as opposed to the 12 pentagons and 12 hexagons that would have been expected of a fullerene structure. Expanding the map (9.81) about $z = 0$ gives

$$R(z) = az + z^5(7a^2 - 32a - 39) + \cdots , \tag{9.82}$$

and since $|a| > 1$, a comparison with Eq. (9.79) confirms that the point $z = 0$ is a tetravalent vertex. The $B = 9$ minimizing map also contains tetravalent vertices (this time two of them) and this can be checked in a similar way.

A more global characterization of the vertices would be useful. Usually they correspond to local maxima of the integrand defining $\mathcal{I}$ in Eq. (9.63). This density depends on the modulus of the rational map and its derivative, but there is generally no simple formula for finding its maxima. However, in particularly symmetric cases the vertices can be identified with the zeros of the Hessian. Explicitly, the Hessian is the polynomial

$$H(z) = (2B - 2)W(z)W''(z) - (2B - 3)W'(z)^2 , \tag{9.83}$$

where $W(z)$ is the Wronskian. It has degree $4(B-2)$, which is consistent with the GEM rule for the number of vertices. For example, for the

icosahedral rational map describing the minimal energy $B = 7$ Skyrmion.

$$R(z) = \frac{z^7 - 7z^5 - 7z^2 - 1}{z^7 + 7z^5 - 7z^2 + 1}, \tag{9.84}$$

the Hessian is

$$H(z) = -8624(z^{20} - 228z^{15} + 494z^{10} + 228z^5 + 1), \tag{9.85}$$

which is proportional to the Klein polynomial $\mathcal{Y}_f$ associated with the vertices of a dodecahedron [237].

9.7 Lattices, crystals and shells

So far we have only discussed Skyrmions with a finite baryon number, but in fact the lowest known value for the energy per baryon, E/B, occurs for an infinite crystal of Skyrmions. As we have seen, for certain relative orientations, well separated Skyrmions attract. At high density it is expected that the Skyrmions will form a crystal, though a crystal structure has not yet been seen dynamically for a finite baryon number, probably due to the fact that so far only simulations up to $B = 22$ have been performed.

To study Skyrmion crystals one imposes periodic boundary conditions on the Skyrme field and works within a unit cell (equivalently, 3-torus) $\mathbb{T}^3$. The first attempted construction of a crystal was by Klebanov [235], using a simple cubic lattice of Skyrmions whose symmetries maximize the attraction between nearest neighbours. After relaxation, Klebanov's crystal has an energy 1.08 per baryon. Other symmetries were proposed which lead to slightly lower, but not minimal, energy crystals [160, 221]. Following the work of Castillejo *et al.* [75] and Kugler and Shtrikman [248], it is now understood that it is best to arrange the Skyrmions initially as a face-centred cubic lattice, with their orientations chosen symmetrically to give maximal attraction between all nearest neighbours. Explicitly, the Skyrme field is strictly periodic after translation by $2L$ in the x^1, x^2 or x^3 directions. A unit cell is a cube of side length $2L$, with Skyrmions in standard orientation on the vertices, and further Skyrmions at the face centres, each rotated by 180° about the axis which is normal to the face. With this set-up each Skyrmion has twelve nearest neighbours which are all in the attractive channel. Inside one unit cell, the total baryon number is $B = 4$. If we fix the origin at the centre of one of the unrotated Skyrmions, this configuration has the combined spatial plus isospin symmetries generated by

$$(x^1, x^2, x^3) \mapsto (-x^1, x^2, x^3), \ (\sigma, \pi_1, \pi_2, \pi_3) \mapsto (\sigma, -\pi_1, \pi_2, \pi_3); \tag{9.86}$$

$$(x^1, x^2, x^3) \mapsto (x^2, x^3, x^1)\,,\ (\sigma, \pi_1, \pi_2, \pi_3) \mapsto (\sigma, \pi_2, \pi_3, \pi_1)\,; \tag{9.87}$$

$$(x^1, x^2, x^3) \mapsto (x^1, x^3, -x^2)\,,\ (\sigma, \pi_1, \pi_2, \pi_3) \mapsto (\sigma, \pi_1, \pi_3, -\pi_2)\,; \tag{9.88}$$

$$(x^1, x^2, x^3) \mapsto (x^1 + L, x^2 + L, x^3)\,,\ (\sigma, \pi_1, \pi_2, \pi_3) \mapsto (\sigma, -\pi_1, -\pi_2, \pi_3)\,. \tag{9.89}$$

Symmetry (9.86) is a reflection in a face of the cube, (9.87) is a rotation around a three-fold axis along a diagonal, (9.88) is a four-fold rotation around an axis through opposite face centres, and (9.89) is a translation from the corner of the cube to a face centre.

At low densities (large L), the Skyrmions are localized around their lattice positions, each having an almost spherical isosurface where $\sigma = 0$, separating the core of the Skyrmion ($\sigma < 0$) from its tail ($\sigma > 0$). Since the Skyrmions are well separated, the average value of σ in a unit cell, $\langle\sigma\rangle$, is close to one.

As the density is increased (that is, L reduced) the energy decreases and there is a phase transition to a crystal of half-Skyrmions. At this point the symmetry is increased by the addition of the generator

$$(x^1, x^2, x^3) \mapsto (x^1 + L, x^2, x^3)\,, \quad (\sigma, \pi_1, \pi_2, \pi_3) \mapsto (-\sigma, -\pi_1, \pi_2, \pi_3)\,, \tag{9.90}$$

a translation half-way along the cube edge. Note that this symmetry involves a chiral $SO(4)$ rotation, rather than just an $SO(3)$ isospin transformation as before. The previous translational symmetry (9.89) can be obtained by applying this new generator, together with this generator rotated by 90°.

This phase is where the minimal energy Skyrme crystal occurs. The $\sigma < 0$ and $\sigma > 0$ regions are perfect cubes of side length L, with $\sigma = 0$ on all the faces. Each cube has identical pion field distributions and baryon number $\frac{1}{2}$. For this configuration, $\langle\sigma\rangle = 0$, and there is a restoration of chiral symmetry. The minimum of the energy occurs at $L \approx 4.7$. A variational method, based on a truncated Fourier series expansion of the fields, approximates the energy per baryon to be $E/B = 1.038$, and a recent numerical calculation [42], using far larger grids than previous studies [75], gives a very similar value of $E/B = 1.036$. In Fig. 9.6 we plot a baryon density isosurface for the Skyrme crystal. Each lump represents a half-Skyrmion and the total baryon number shown is 4. The fields obtained either numerically, or by optimizing the Fourier series, are very well approximated by the analytic formulae [75]

$$\sigma = c_1 c_2 c_3\,, \tag{9.91}$$

$$\pi_1 = -s_1\sqrt{1 - \frac{s_2^2}{2} - \frac{s_3^2}{2} + \frac{s_2^2 s_3^2}{3}} \qquad \text{and cyclic}\,, \tag{9.92}$$

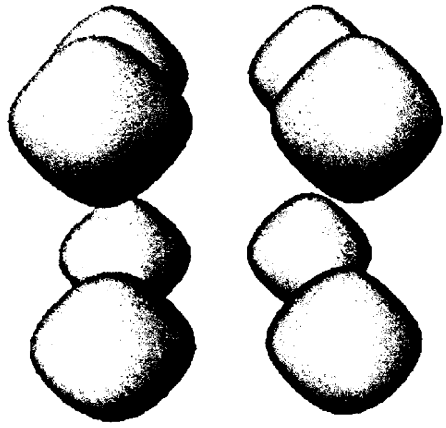

Fig. 9.6. A baryon density isosurface for a portion of the Skyrme crystal.

where $s_i = \sin(\pi x^i/L)$ and $c_i = \cos(\pi x^i/L)$. This approximation to the Skyrme crystal field has the right symmetries and is motivated by an exact solution for a crystal in the two-dimensional $O(3)$ sigma model, which has a similar form but with the trigonometric functions replaced by Jacobi elliptic functions.

Table 9.5 shows that the energy per baryon of the shell-like Skyrmions is decreasing as B increases, but is still some way above that of the Skyrme crystal. The asymptotic value of E/B for the shell-like structures for large B can be compared with the value for the crystal by studying yet another periodic arrangement of Skyrmions, a two-dimensional lattice, rather than a three-dimensional crystal.

In very large fullerenes, where hexagons are dominant, the twelve pentagons may be viewed as defects inserted into a flat structure, to generate the curvature necessary to close the shell. Energetically, the optimum infinite structure is a hexagonal lattice, that is, a graphite sheet – the most stable form of carbon thermodynamically. The reason that closed shells are preferred for a finite number of carbon atoms is that the penalty for introducing the pentagonal defects is not as severe as that incurred by having dangling bonds at the edges of a truncated graphite sheet. A prediction of the fullerene approach to Skyrmions is the existence of a Skyrme field analogous to a graphite sheet. This configuration would have infinite energy, since it has infinite extent in two directions, but its energy per baryon should be lower than that of any of the known finite energy Skyrmions, and will be the asymptotic value approached by large fullerene-like Skyrmions.

Such a hexagonal Skyrme lattice can be constructed using the ansatz of ref. [42]

$$U(x^1,x^2,x^3)=\exp\left(\frac{if}{1+|R|^2}(R\tau_-+\bar{R}\tau_++(1-|R|^2)\tau_3)\right), \qquad (9.93)$$

a variant of the rational map ansatz. Here $\tau_\pm=\tau_1\pm i\tau_2$, R is a meromorphic, periodic function of $z=x^1+ix^2$, and f is a real function of x^3 chosen so that the Skyrme lattice physically occupies the (x^1,x^2) plane. The direction of the vector of pion fields is determined by $R(z)$, whereas the magnitude of the vector also depends on the profile function f, and hence on the height above or below the lattice. If Ω_1 and Ω_2 are the fundamental periods of $R(z)$, then

$$U(z+n\Omega_1+m\Omega_2,x^3)=U(z,x^3)\quad\forall\, n,m\in\mathbb{Z}. \qquad (9.94)$$

Let $\mathbb{T}^2$ denote the associated torus, the parallelogram in the complex plane with vertices $0,\Omega_1,\Omega_2,\Omega_1+\Omega_2$ and opposite edges identified.

To understand the boundary conditions on f we need to recall our motivation. The lattice is being thought of as an infinite limit of the shell-like Skyrmions containing pentagons and hexagons. Thus, below the lattice is the outside of the shell, where $U\to 1_2$. Above the lattice is the inside of the shell, where the Skyrme field is approaching the value associated with the centre of the Skyrmion, so $U\to -1_2$. We therefore require

$$f(-\infty)=0,\ f(\infty)=\pi. \qquad (9.95)$$

This implies that the Skyrme lattice is a novel domain wall, separating differing vacua.

To compute the baryon number and energy of the Skyrme field (9.93) it is again convenient to use the geometrical strain formulation. The strain in the direction normal to the lattice is orthogonal to the two strains tangential to the lattice, which are equal. λ_i may be interpreted as the strain in the x^i direction, and it is easy to show that

$$\lambda_1=\lambda_2=2J\sin f,\quad \lambda_3=f', \qquad (9.96)$$

where

$$J=\frac{1}{1+|R|^2}\left|\frac{dR}{dz}\right|. \qquad (9.97)$$

Therefore, the energy and baryon densities (9.12) are

$$\mathcal{E}=\frac{1}{12\pi^2}\left(f'^2+8J^2(f'^2+\sin^2 f)+16J^4\sin^4 f\right), \qquad (9.98)$$

$$\mathcal{B}=\frac{2}{\pi^2}J^2f'\sin^2 f. \qquad (9.99)$$

We now compute the baryon number B in a fundamental region of the lattice, $x^3 \in (-\infty, \infty)$ and $(x^1, x^2) \in \mathbb{T}^2$. Since R is a map from $\mathbb{T}^2$ to S^2, its degree, k, is the integral over $\mathbb{T}^2$ of the pull-back of the area 2-form on S^2, $dRd\bar{R}/(1+|R|^2)^2$, that is

$$k = \frac{1}{\pi}\int_{\mathbb{T}^2} J^2\, dx^1 dx^2\,, \tag{9.100}$$

since R is a holomorphic function of z. Using (9.99) it is now easy to see that the baryon number is equal to the degree k, since

$$B = \frac{2}{\pi^2}\int_{-\infty}^{\infty} f' \sin^2 f\, dx^3 \int_{\mathbb{T}^2} J^2\, dx^1 dx^2 = \frac{k}{\pi}\Big[f - \frac{1}{2}\sin 2f\Big]_{-\infty}^{\infty} = k\,. \tag{9.101}$$

using (9.100) and the boundary conditions (9.95).

To calculate the energy E in the fundamental region it is useful to introduce a scale parameter μ, write $u = x^3/\mu$ and set $f(x^3) = g(u)$. Then, if A is the area of the fundamental torus $\mathbb{T}^2$, integrating the density (9.98) gives

$$E = \int_{-\infty}^{\infty} dx^3 \int_{\mathbb{T}^2} \mathcal{E}\, dx^1 dx^2 \;= \frac{A}{\mu}E_1 + \frac{1}{\mu}E_2 + \mu E_3 + \frac{\mu}{A}E_4\,, \tag{9.102}$$

where

$$\begin{aligned} E_1 &= \frac{1}{12\pi^2}\int_{-\infty}^{\infty} g'^2\, du\,, \quad E_2 = \frac{2k}{3\pi}\int_{-\infty}^{\infty} g'^2 \sin^2 g\, du\,, \\ E_3 &= \frac{2k}{3\pi}\int_{-\infty}^{\infty} \sin^2 g\, du\,. \quad E_4 = \frac{4\mathcal{I}}{3\pi^2}\int_{-\infty}^{\infty} \sin^4 g\, du\,. \end{aligned} \tag{9.103}$$

E depends on the map R only through the quantity

$$\mathcal{I} = A\int_{\mathbb{T}^2} J^4\, dx^1 dx^2\,, \tag{9.104}$$

a combination independent of A. The scale μ and area A are fixed in terms of the E_i's, by minimizing (9.102). Requiring $\frac{\partial E}{\partial \mu} = \frac{\partial E}{\partial A} = 0$ gives

$$\mu = \sqrt{E_2/E_3}\,, \quad A = \sqrt{E_2 E_4/E_1 E_3}\,, \tag{9.105}$$

and hence the minimized energy is

$$E = 2(\sqrt{E_1 E_4} + \sqrt{E_2 E_3})\,. \tag{9.106}$$

To proceed further we choose $R(z)$ to be an elliptic function with a hexagonal period lattice. The simplest is the Weierstrass function $\wp(z)$ satisfying

$$\wp'^2 = 4(\wp^3 - 1)\,. \tag{9.107}$$

which has periods $\Omega_1 = \Gamma(\frac{1}{6})\Gamma(\frac{1}{3})/(2\sqrt{3\pi})$ and $\Omega_2 = \Omega_1 \exp(\pi i/3)$. Obviously we can scale both the elliptic function and its argument and still have a hexagonal period lattice; hence we take

$$R(z) = c\wp(z/\alpha)\,, \tag{9.108}$$

where c and α are arbitrary real constants. For computational purposes it is actually more convenient to work with a rectangular fundamental torus, $(x^1, x^2) \in [0, \alpha\Omega_1] \times [0, \alpha\sqrt{3}\Omega_1]$, whose area is $A = \sqrt{3}\alpha^2\Omega_1^2$. As this torus contains two fundamental parallelograms and the $\wp$-function has one double pole in each, then by counting preimages, we see that the degree of the map from the rectangular torus to the sphere is $k = 4$.

E is minimized by choosing c so as to minimize $\mathcal{I}$. The minimal value is $\mathcal{I} \approx 193$, when $c \approx 0.7$. (Recall that $\mathcal{I}$ is independent of α.)

We now make the simplifying ansatz that $g(u)$ is the sine-Gordon kink profile function

$$g(u) = 2\tan^{-1} e^u\,, \tag{9.109}$$

which is a reasonably good choice, and has the advantage that all the integrals in (9.103) can be performed exactly. The results are

$$E_1 = \frac{1}{6\pi^2}\,,\quad E_2 = \frac{32}{9\pi}\,,\quad E_3 = \frac{16}{3\pi}\,,\quad E_4 = \frac{16\mathcal{I}}{9\pi^2}\,, \tag{9.110}$$

from which we find that the scale and area are

$$\mu = \sqrt{\frac{2}{3}}\,,\quad A = \frac{8}{3}\sqrt{\mathcal{I}}\,, \tag{9.111}$$

and using (9.106), that the energy is

$$E = \frac{4}{3\pi^2}\sqrt{\frac{2}{3}}(\sqrt{\mathcal{I}} + 8\pi)\,. \tag{9.112}$$

Recalling the numerical value of $\mathcal{I}$, and that $B = k = 4$, we thus find an energy per baryon

$$E/B = 1.076\,. \tag{9.113}$$

The true lattice has been determined by numerical relaxation, using the ansatz above, involving the Weierstrass function and sine-Gordon kink profile, to give a starting approximation [42]. Its energy is found to be

$$E/B = 1.061\,. \tag{9.114}$$

In Fig. 9.7 we display a surface of constant baryon density for this hexagonal Skyrme lattice. The structure is clearly visible, the baryon density

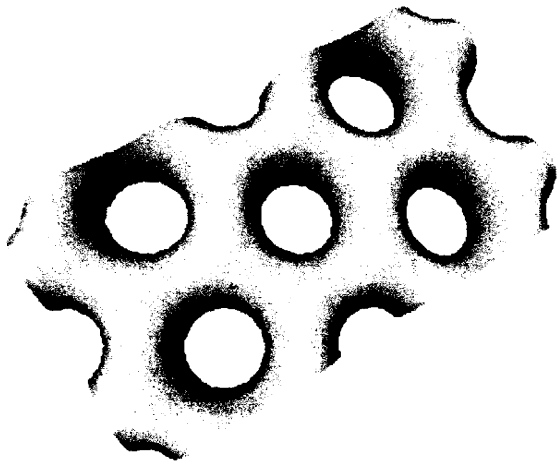

Fig. 9.7. A baryon density isosurface for a portion of the Skyrme lattice.

having a hole in the centre of each of the hexagonal faces. Note that the displayed region contains exactly eight full hexagons and has baryon number 4, so each hexagon may be thought of as having baryon number $\frac{1}{2}$. This is the expected limit of the polyhedron structures discussed earlier, where a charge B Skyrmion has $2(B-1)$ faces. Other lattices, such as a tetravalent square lattice, can be created by choosing a Weierstrass function different from (9.107), but these have energies which are slightly higher than the trivalent hexagonal lattice.

Since the energy per baryon of the Skyrme lattice exceeds that of the Skyrme crystal it is reasonable to expect that above some critical charge, the minimal energy Skyrmion will resemble a portion of the crystal rather than a shell constructed from the planar lattice by inserting pentagonal defects. As the crystal is basically a stack of $B = 4$ cubes, $B = 32$ is the first charge at which any sizeable, symmetric chunk of the crystal can emerge. Attempts have been made [35] to construct Skyrme fields by cutting out a portion of the crystal and interpolating its surface fields to the vacuum, but these all have rather high energies.

An alternative to either a single-shell or crystal structure is a two-shell structure. This has been investigated [290] using yet another variant of the rational map ansatz,

$$U(r,z) = \exp(\theta(r_0-r)if_1(r)\hat{\mathbf{n}}_{R_1(z)}\cdot\boldsymbol{\tau}+\theta(r-r_0)if_2(r)\hat{\mathbf{n}}_{R_2(z)}\cdot\boldsymbol{\tau}), \quad (9.115)$$

where $\theta(r)$ is the Heaviside step function and r_0 is a radius where the two shells meet. The two profile functions, f_1 and f_2, satisfy the boundary

conditions $f_1(0) = 2\pi$, $f_1(r_0) = f_2(r_0) = \pi$, $f_2(\infty) = 0$, and the angular distributions of the fields on the two shells are determined by two rational maps R_1 and R_2, with degrees k_1 and k_2 respectively. The baryon number of this configuration is $B = k_1 + k_2$. The multi-shell generalization is obvious.

Some two-shell and three-shell configurations for $B = 12, 13, 14$ have been studied, and also used as initial configurations in a numerical relaxation of the full Skyrme energy. In most cases they relax to a single-shell structure, with energy a bit higher than that described in Section 9.6, so they probably describe saddle points. Note that two-shell configurations have $U = 1_2$ at the origin, so can not relax to the minimal energy single-shell Skyrmions discussed in Section 9.6, for which $U = -1_2$ there.

The two-shell ansatz with baryon number $k_1 + k_2$ has an interpretation in terms of $k_1 + k_2$ individual Skyrmions on a single shell, which is often the end point of a numerical relaxation. To see this, consider $U(r, z)$ for a given value of z, and compare the values of U at the two radii where $f_1(r) = \frac{3}{2}\pi$ and $f_2(r) = \frac{1}{2}\pi$. If these values are close, the field configuration along this radial line can be relaxed to be approximately constant, but if they are antipodal then the radial gradient energy is large and may be interpreted as due to a single Skyrmion at $r = r_0$, with angular location z. The condition that the values of U are antipodal is that $R_1(z) = R_2(z)$, since the rational maps then have the same value but the profile functions have opposite sign, that is, $\sin f_1 = -1$, $\sin f_2 = 1$. If $R_1 = p_1/q_1$ and $R_2 = p_2/q_2$ then the antipodal condition is

$$p_1(z)q_2(z) - p_2(z)q_1(z) = 0\,, \tag{9.116}$$

which is a polynomial equation of degree $k_1 + k_2$. The $k_1 + k_2$ roots determine the angular locations of the Skyrmions on the shell $r = r_0$.

In summary, there are a number of alternatives to a single-shell structure for Skyrmions and what is remarkable is that none of these alternatives appears to give minimal energy Skyrmions for $B \leq 22$. However, single-shells can not be the whole story for large enough baryon number.

9.8 Skyrmion dynamics

In the preceding sections we have been concerned with static Skyrmions, but in this section we turn to Skyrmion dynamics and scattering. To begin with, we describe how some of the static, symmetric, minimal energy Skyrmions can be formed from the collision of well separated single Skyrmions [40].

The time dependent Skyrme field equation is solved using a finite difference method (see ref. [45] for a detailed discussion), which is most

conveniently implemented using a nonlinear sigma model formulation. Explicitly, the Skyrme field is parametrized by the unit 4-vector $\phi = (\sigma, \pi_1, \pi_2, \pi_3)$, in terms of which the Lagrangian density becomes

$$\mathcal{L} = \partial_\mu \phi \cdot \partial^\mu \phi - \tfrac{1}{2}(\partial_\mu \phi \cdot \partial^\mu \phi)^2 + \tfrac{1}{2}(\partial_\mu \phi \cdot \partial_\nu \phi)(\partial^\mu \phi \cdot \partial^\nu \phi) + \lambda(\phi \cdot \phi - 1), \quad (9.117)$$

with the Lagrange multiplier λ introduced in order to enforce the constraint $\phi \cdot \phi = 1$.

The Euler-Lagrange equation is

$$\begin{aligned}(1 - \partial_\mu \phi \cdot \partial^\mu \phi)\partial_\alpha \partial^\alpha \phi \quad &- \quad (\partial^\nu \phi \cdot \partial_\mu \partial_\nu \phi - \partial_\mu \phi \cdot \partial_\alpha \partial^\alpha \phi)\partial^\mu \phi \\ &+ \quad (\partial^\mu \phi \cdot \partial^\nu \phi)\partial_\mu \partial_\nu \phi - \lambda \phi = 0, \quad (9.118)\end{aligned}$$

where λ can be calculated by contracting (9.118) with ϕ and using the second derivative of the constraint, giving

$$\lambda = -(\partial_\mu \phi \cdot \partial_\nu \phi)(\partial^\mu \phi \cdot \partial^\nu \phi) - (1 - \partial_\mu \phi \cdot \partial^\mu \phi)\partial_\nu \phi \cdot \partial^\nu \phi. \quad (9.119)$$

The simplest possible scattering event involves the head-on collision of two Skyrmions in the attractive channel. As discussed in Section 9.3, an initial configuration can be constructed using the product ansatz $U = U^{(1)}U^{(2)}$ for well separated Skyrmions, each of which may also be independently Lorentz boosted. An example that has been calculated has an initial configuration consisting of two Skyrmions with positions

$$\mathbf{X}_1 = (0, 0, a), \quad \mathbf{X}_2 = (0, 0, -a), \quad (9.120)$$

where $a = 1.5$; the second Skyrmion is rotated relative to the first by a 180° rotation around the x^2-axis, and each Skyrmion is Lorentz boosted towards the other with a velocity $v = 0.3$, in order to speed up the interaction.

Figure 9.8 shows an isosurface plot of the baryon density at regular time intervals. We see that the initially well separated Skyrmions deform as they come together, before coalescing into a toroidal configuration very close to the exact minimal energy $B = 2$ Skyrmion. The torus then breaks up, with the result that the Skyrmions scatter at right angles. This right-angle scattering was predicted analytically [283] and is a familiar property of two-soliton scattering; for example, we have already seen that monopoles and vortices exhibit this behaviour. The Skyrmions then attract once more and pass through the torus again. This almost elastic process repeats itself a number of times, with a little energy being radiated each time, eventually settling down to the exact static solution.

In order to discuss attractive configurations of $B > 2$ Skyrmions we first introduce some notation. Take the positions of the single Skyrmions to be $\mathbf{X}_i$ for $i = 1, \ldots, B$, and define the relative position vectors $\mathbf{X}_{ij} = \mathbf{X}_i - \mathbf{X}_j$.

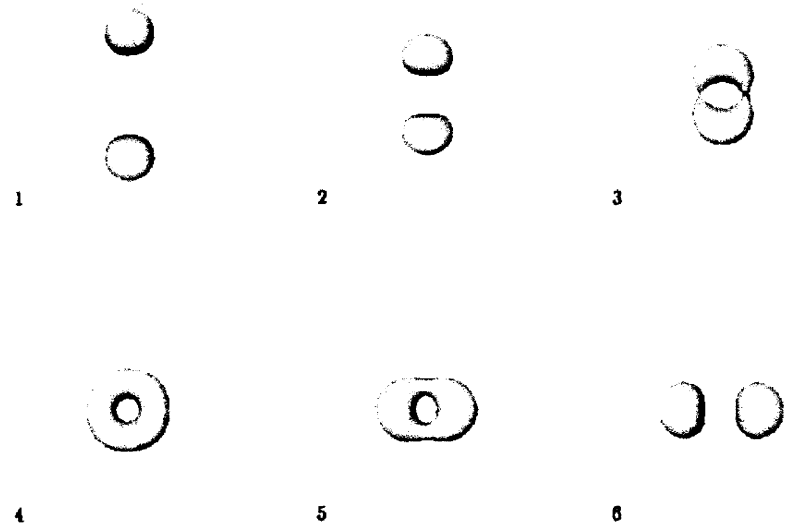

Fig. 9.8. Baryon density isosurfaces at increasing times during the head-on collision of two Skyrmions.

Suppose the orientation of the Skyrmion at $\mathbf{X}_i$ relative to that at $\mathbf{X}_j$ is obtained by a rotation by 180° about an axis with unit vector $\mathbf{n}_{ij}$. Then all pairs will mutually, maximally attract if $\mathbf{X}_{ij} \cdot \mathbf{n}_{ij} = 0$ (no sum) for all $i \neq j$.

Three Skyrmions can scatter close to the tetrahedral $B = 3$ Skyrmion. In choosing Skyrmion initial configurations, the analogous monopole scattering is a good guide. Recall from Chapter 8 that the tetrahedral 3-monopole is formed during the C_3-symmetric scattering in which three monopoles are initially on the vertices of a large contracting equilateral triangle. We therefore take three well separated Skyrmions in such a configuration, with

$$\mathbf{X}_1 = (-a, -a, -a), \quad \mathbf{X}_2 = (-a, a, a), \quad \mathbf{X}_3 = (a, -a, a). \tag{9.121}$$

The first Skyrmion is in standard orientation, and the orientations of the second and third are fixed by taking

$$\mathbf{n}_{12} = (1, 0, 0), \quad \mathbf{n}_{13} = (0, 1, 0). \tag{9.122}$$

This implies that $\mathbf{n}_{23} = (0, 0, 1)$, so all pairs are in the attractive channel, since $\mathbf{X}_{ij} \cdot \mathbf{n}_{ij} = 0$ for all $i \neq j$.

Again we choose $a = 1.5$, and this time each Skyrmion is boosted to have an initial velocity of $v = 0.17$ towards the centre of the triangle. The evolution of this configuration is shown in Fig. 9.9.

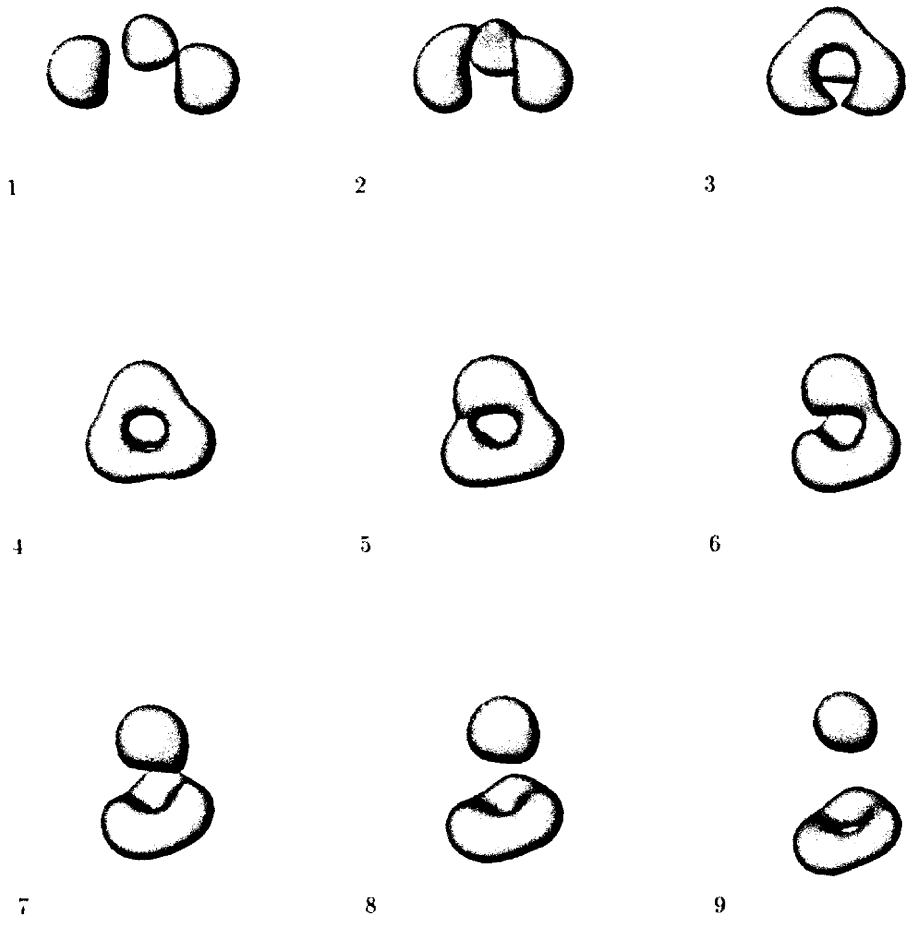

Fig. 9.9. Baryon density isosurfaces at increasing times during the scattering of three Skyrmions with approximate C_3 symmetry.

We should point out that the C_3 symmetry is slightly broken by the product ansatz implementation of the initial data, $U = U^{(1)}U^{(2)}U^{(3)}$, which is clearly asymmetric under permutations of the indices. If a were larger, the product ansatz would be closer to having exact cyclic symmetry.

The Skyrmions deform as they coalesce, and each behaves slightly differently. The dynamics is, nonetheless, remarkably similar to the monopole case, except for the influence of the varying potential energy, in that the Skyrmions form an approximately tetrahedral configuration, which then splits into a single Skyrmion and a charge 2 torus.

We have seen a second scattering process passing through the tetrahedral 3-monopole - the twisted line scattering of three collinear monopoles. A similar scattering process also occurs for three collinear Skyrmions with appropriate orientations [40].

Recall that four monopoles on the vertices of a contracting regular tetrahedron scatter through the cubic charge 4 solution. There is an analogous four-Skyrmion scattering process. To the $B = 3$ system given by (9.121) and (9.122), we add a fourth Skyrmion at $\mathbf{X}_4 = (a, a, -a)$ with orientation given by $\mathbf{n}_{14} = (0, 0, 1)$. This completes a regular tetrahedron. The additional relative orientations are $\mathbf{n}_{24} = (0, 1, 0)$ and $\mathbf{n}_{34} = (1, 0, 0)$, so still we have $\mathbf{X}_{ij} \cdot \mathbf{n}_{ij} = 0$ for all $i \neq j$, and all Skyrmion pairs maximally attract. Once more we take $a = 1.5$, but this time no initial Lorentz boosts are required, because of the strong attractions.

The evolution of this configuration is displayed in Fig. 9.10. The mutual attractions cause the Skyrmions to coalesce and form a cubic configuration. This then splits up, and the Skyrmions are found on the vertices of a tetrahedron dual to the initial one. Again the product ansatz implementation results in the tetrahedral symmetry being only approximately attained. Aside from this technicality, however, the scattering process is once again a close copy of what happens for monopoles.

Another configuration is four Skyrmions on the corners of the square

$$\mathbf{X}_1 = (a, a, 0)\,,\ \mathbf{X}_2 = (a, -a, 0)\,,\ \mathbf{X}_3 = (-a, -a, 0)\,,\ \mathbf{X}_4 = (-a, a, 0)\,. \tag{9.123}$$

If

$$\mathbf{n}_{12} = (1, 0, 0)\,, \quad \mathbf{n}_{13} = (0, 0, 1)\,, \quad \mathbf{n}_{14} = (0, 1, 0)\,, \tag{9.124}$$

then $\mathbf{n}_{23} = (0, 1, 0)$, $\mathbf{n}_{24} = (0, 0, 1)$, $\mathbf{n}_{34} = (1, 0, 0)$ which implies that all pairs mutually attract. The dynamics of this configuration is exhibited in Fig. 9.11 for initial conditions with no Lorentz boost. The initial D_4-symmetric configuration scatters through the $B = 4$ cube and emerges as two $B = 2$ tori; yet another well known monopole process.

Given that N-monopole dynamics at low energy can be well approximated by geodesic motion on the monopole moduli space, a natural ques-

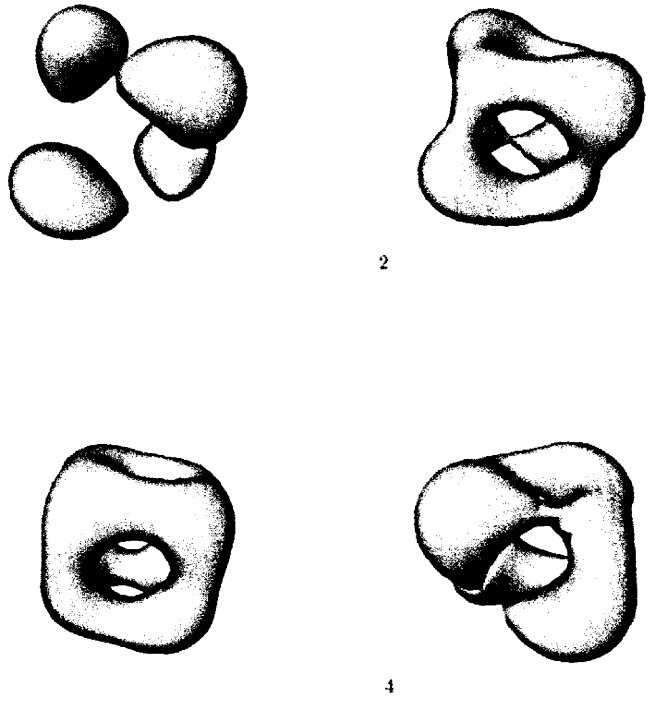

Fig. 9.10. Baryon density isosurfaces at increasing times during the scattering of four Skyrmions with approximate tetrahedral symmetry.

tion is whether a similar moduli space approximation exists for Skyrmions. Since there are weak forces between Skyrmions, the moduli space of the exact minimal energy Skyrmion of charge B does not contain adequate degrees of freedom to describe all the required low energy configurations. It is at most nine-dimensional, corresponding to the action of translations, rotations and isospin rotations on the otherwise unique solution. Another manifold $\mathcal{M}_B$, whose coordinates parametrize a suitably larger set of low energy field configurations, is required. Ideally, $\dim \mathcal{M}_B = 6B$. since this is the dimension of the space of B well separated Skyrmions with all possible orientations.

An obvious candidate for $\mathcal{M}_B$ is the parameter space of field configurations obtained using the product ansatz for B Skyrmions. This is certainly $6B$-dimensional and adequately describes well separated Skyrmions, but it is not acceptable since the product ansatz fails near the minimal energy charge B Skyrmion. For example, the product ansatz for two Skyrmions satisfactorily defines $\mathcal{M}_2$ when the Skyrmion separation is large compared to the Skyrmion size, and the energy initially decreases in the attractive

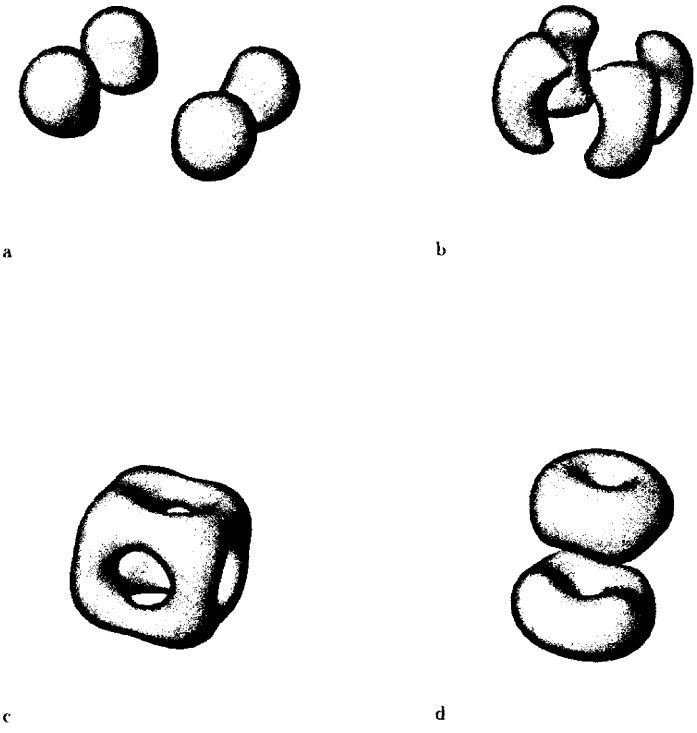

Fig. 9.11. Baryon density isosurfaces at increasing times during the scattering of four Skyrmions with approximate D_4 symmetry.

channel as the separation is reduced, as we have seen from the calculation of the asymptotic interaction energy in Section 9.3. However, as the separation is reduced further the interaction energy obtained from the product ansatz begins to increase [218] and a product of coincident Skyrmions does not resemble the minimal energy $B = 2$ torus.

A more promising definition [284] of $\mathcal{M}_2$ is as the unstable manifold of the spherically symmetric $B = 2$ hedgehog solution, which we discussed in Section 9.2. This saddle point solution may be thought of as two coincident Skyrmions, with one wrapped around the other. (It is also well approximated in the product ansatz by two coincident Skyrmions with the same orientation.) It has six unstable modes, and six zero modes, three translational and three rotational. Of the six unstable modes, three correspond to rotating one of the Skyrmions with respect to the other, while three are associated with separating the Skyrmions. The union of gradient flow curves descending from the $B = 2$ hedgehog in all possible positions and orientations is a 12-dimensional manifold. A generic curve will end at the minimal energy $B = 2$ torus, but a submanifold of curves

will end at infinitely separated Skyrmions. Curves close to this submanifold will go out to well separated Skyrmions and then return to the torus. This definition of $\mathcal{M}_2$ will therefore include well separated Skyrmions in all possible orientations, but it will also include the low energy configurations where the Skyrmions are close together.

An attempt has been made to construct $\mathcal{M}_2$ numerically [409] by solving the gradient flow equation

$$R_0 - \frac{1}{4}[R_i, [R_i, R_0]] = \partial_i (R_i - \frac{1}{4}[R_j, [R_j, R_i]]) \,. \tag{9.125}$$

Particularly interesting is one of the steepest and shortest gradient flow trajectories, where the constituent Skyrmions of the hedgehog simultaneously separate a little, and twist, then recombine into the torus. A systematic construction of some two-dimensional submanifolds of $\mathcal{M}_2$ has been carried out, and with the action of the nine-dimensional symmetry group this is effectively a construction of some 11-dimensional submanifolds of $\mathcal{M}_2$. The 10-dimensional attractive channel of two Skyrmions has also been found using the gradient flow, starting with well separated Skyrmions. However, it is difficult numerically to implement gradient flow in regions where the Skyrmions are well separated. As a technical simplification, in this region the product ansatz can be used. In fact for well separated Skyrmions the gradient flow equations within the product ansatz can be solved exactly [211]. In conclusion, the work in [409] and [211] shows that it is feasible, if difficult, to construct $\mathcal{M}_2$ using numerical gradient flow.

Given the manifold $\mathcal{M}_2$ one can now attempt to define a truncated dynamics on it by restriction of the Skyrme Lagrangrian. Note that, unlike the moduli space approximation for monopoles, there will be both a non-trivial metric and potential energy function on $\mathcal{M}_2$. These have been partly calculated in ref. [409]. The potential is easy to calculate along any gradient flow curve. The metric coefficient along a gradient flow curve can be inferred from the rate at which the potential energy decreases. Several of the remaining metric coefficients are (spin and isospin) moments of inertia of the configurations generated during the gradient flow. The topography of $\mathcal{M}_2$ is a valley within the infinite-dimensional configuration space of $B = 2$ Skyrme fields, with the attractive channel being an almost flat submanifold of this. The highest point in $\mathcal{M}_2$ is the $B = 2$ hedgehog, whose energy is about one and a half times that of either the torus or well separated Skyrmions. So at really low energies the region near the hedgehog will not be explored, even though this is the solution on which the whole construction of $\mathcal{M}_2$ is based. The fact that the valley is not precisely flat, because of the weak inter-Skyrmion forces, means that the motion can not be assumed to be vanishingly slow. For example, the

attraction of two Skyrmions may build up modest speeds even if they start at rest.

In principle, $\mathcal{M}_B$ could be the unstable manifold of the charge B hedgehog solution. The product ansatz suggests that this solution has $6B-6$ unstable modes and six zero modes. However, a practical implementation is even less feasible.

In the simpler case of a (2+1)-dimensional Baby Skyrme model, a rather differently defined moduli space involving both a metric and a potential function has been constructed to study the classical dynamics of two solitons [388], and yields results which are in good agreement with full field simulations. The Baby Skyrme model may be considered as a deformation of the $O(3)$ sigma model, for which a precisely defined moduli space, $\mathcal{M}$, of static Bogomolny lump solutions exists. $\mathcal{M}$, with a deformed metric, is a suitable approximate moduli space for the deformed theory. The potential is approximated by evaluating the energy of sigma model lumps using the Baby Skyrmion potential energy function. Unfortunately the Skyrme model can not be treated in this way as there is no known deformation of the model to a nearby one with Bogomolny equations.

A related aspect of Skyrmion dynamics is of interest, namely, an analysis of the vibrational modes of minimal energy Skyrmions. This leads to a model of the linearization of the moduli space $\mathcal{M}_B$, near the Skyrmion. The low frequency vibrational modes provide a coordinate independent description of the configuration space around the static solution. Calculating the frequencies of the lowest-lying vibrational modes also provides a first step in an attempt to quantize the Skyrmion within a harmonic approximation. We will not discuss the quantization aspect, but we will discuss how the vibrational modes of Skyrmions provide yet another link to monopoles.

A numerical computation of the vibration frequencies, and the classification of degenerate modes into irreducible representations of the symmetry group of the static Skyrmion, has been performed for charges $B=2$ and $B=4$ [34], and a qualitative analysis has been given for $B=7$ [36]. The method employed is to solve a semi-linearized form of the time dependent Skyrme equation, with as initial condition a rather general, slightly perturbed Skyrmion. The frequencies of the normal modes are found by Fourier transforming the fields at a given spatial location with respect to time. The spectrum obtained can be divided into two parts, corresponding to vibration frequencies below and above that of the breather mode, which is the oscillation corresponding to a change in the scale size of the Skyrmion. We are more interested in the lower-lying modes below the breather, since they can be identified with variations of the parameters in the rational map describing the static Skyrmion.

To be specific, let us consider the vibrations of the cubic $B=4$ Skyrmion, whose modes lie in multiplets transforming under real irre-

ducible representations of the octahedral group O. The computations of ref. [34] reveal that there are nine modes below the breather, which transform under the representations E, A_1, F_2, F_2, in order of increasing frequency.

Recall that the rational map of degree 4 with octahedral symmetry is

$$R_0(z) = \frac{z^4 + 2\sqrt{3}iz^2 + 1}{z^4 - 2\sqrt{3}iz^2 + 1}. \tag{9.126}$$

The general variation of this map, in which we preserve the leading coefficient, 1, of the numerator as a normalization, is

$$R(z) = \frac{z^4 + \alpha z^3 + (2\sqrt{3}i + \beta)z^2 + \gamma z + 1 + \delta}{(1+\lambda)z^4 + \mu z^3 + (-2\sqrt{3}i + \nu)z^2 + \sigma z + 1 + \tau} \tag{9.127}$$

where $\alpha, \beta, \gamma, \delta, \lambda, \mu, \nu, \sigma, \tau$ are small complex numbers. We now calculate the effect of the transformations of the octahedral group. For example, the 90° rotation, represented by the transformation $R(z) \mapsto 1/R(iz)$ leaves R_0 fixed, but transforms the more general map $R(z)$ to

$$\tilde{R}(z) = \frac{(1+\lambda)z^4 - i\mu z^3 + (2\sqrt{3}i - \nu)z^2 + i\sigma z + 1 + \tau}{z^4 - i\alpha z^3 - (2\sqrt{3}i + \beta)z^2 + i\gamma z + 1 + \delta}. \tag{9.128}$$

Normalizing this by dividing top and bottom by $1 + \lambda$, and ignoring quadratic and smaller terms in the small parameters, we get

$$\tilde{R}(z) = \frac{z^4 - i\mu z^3 + (2\sqrt{3}i - \nu - 2\sqrt{3}i\lambda)z^2 + i\sigma z + 1 + \tau - \lambda}{(1-\lambda)z^4 - i\alpha z^3 + (-2\sqrt{3}i - \beta + 2\sqrt{3}i\lambda)z^2 + i\gamma z + 1 + \delta - \lambda}. \tag{9.129}$$

Hence, the transformation acts linearly on the nine parameters $\alpha, \ldots, \tau$ via a complex 9×9 representation matrix that can be read off from this expression. As we want to deal with a real representation, we consider this as a real 18×18 matrix. The only contribution to the trace of this matrix is associated with the replacement of λ by $-\lambda$ in the leading term of the denominator. Since λ has a real and imaginary part, the character of the 90° rotation in this representation is -2.

Similar calculations for elements of each conjugacy class of the octahedral group give the remaining characters and allow us to identify the irreducible content of this representation as $2A_1 \oplus 2E \oplus 2F_1 \oplus 2F_2$.

To determine which of these irreducible representations correspond to true vibrations we need to remove those corresponding to zero modes. To find the zero mode representation associated with isospin rotations of the Skyrme field, we consider the infinitesimal $SU(2)$ Möbius deformations

$$R_0(z) \mapsto \frac{(1+i\varepsilon)R_0(z) + \varepsilon'}{-\bar{\varepsilon}' R_0(z) + (1 - i\varepsilon)} \tag{9.130}$$

where ε is real, and ε' complex. Under the transformations of the octahedral group a computation of the characters reveals that these variations transform as $A_1 \oplus E$. Similarly, the variations which correspond to translations and rotations transform under the octahedral group as $F_1 \oplus F_1$. From the above 18-dimensional representation we therefore remove $A_1 \oplus E \oplus F_1 \oplus F_1$ to obtain the representation of the true vibrations. This has the irreducible components $A_1 \oplus E \oplus F_2 \oplus F_2$, and is nine-dimensional. These irreducible representations are precisely the ones obtained from the Fourier analysis of the field vibrations, given earlier.

As we saw, a number of scattering events through the symmetric minimal energy Skyrmions have a remarkable similarity to monopole scatterings. These monopole-like, Skyrmion scattering processes correspond precisely to the extension of the low-lying vibrational modes (which we refer to as monopole modes) to large amplitude, splitting the minimal energy Skyrmion into clusters of lower charge. Each monopole mode corresponds to a different cluster decomposition and it is often possible to identify the correspondence by comparing the symmetries of the scattering process and the vibration mode. A more sophisticated approach is to use the irreducible representation of each vibration mode to identify the mode with an explicit rational map deformation. Via the Jarvis correspondence between monopoles and rational maps, the extension of this deformation to large parameter values determines a monopole configuration with well separated clusters. The cluster decomposition of the Skyrmion can thus be identified.

As an example, the one-dimensional A_1 mode in the vibrational spectrum of the $B = 4$ Skyrmion is represented by the 1-parameter family of rational maps

$$R(z) = c\frac{z^4 + 2\sqrt{3}iz^2 + 1}{z^4 - 2\sqrt{3}iz^2 + 1}, \tag{9.131}$$

with c close to 1. Extending c to arbitrary positive values, and using the Jarvis correspondence, we recognize this family of tetrahedrally symmetric maps as describing the dynamics of four monopoles which approach and separate on the vertices of dual tetrahedra and pass through the cubic 4-monopole. Therefore this vibrational mode, extended to large amplitude, will separate the $B = 4$ Skyrmion into four single Skyrmions on the vertices of a tetrahedron, which is one of the attractive channel scatterings that we have already discussed. We denote this process by $1 + 1 + 1 + 1$ to signify the charges of the clusters into which the Skyrmion separates. The other $B = 4$ attractive channel scattering we have considered is the D_4-symmetric scattering, which emerges as $2 + 2$, that is, two $B = 2$ tori. This cluster decomposition corresponds to the two-dimensional vibrational representation E. The two remaining three-dimensional repre-

sentations correspond to the cluster decompositions $3+1$, in which a single Skyrmion collides with the tetrahedral $B = 3$ Skyrmion preserving cyclic C_3 symmetry throughout, and the final decomposition is $2+1+1$, which is a D_{3d} twisted line scattering in which two single Skyrmions collide symmetrically with a $B = 2$ torus. All these scattering processes have been computed using full field simulations, verifying the above picture.

The Jarvis rational maps of degree B have $4B + 2$ parameters. For general B one therefore expects the minimal energy Skyrmion to have $4B - 7$ monopole vibrational modes below the breather, where the nine zero modes describing translations, rotations and isospin rotations have been subtracted off. As another example, for the $B = 3$ tetrahedral Skyrmion, there are five monopole modes, and a rational map symmetry analysis [193] suggests that they form an irreducible doublet and triplet of the tetrahedral group. The two distinct modes correspond to the two possible cluster decompositions, $2+1$ and $1+1+1$, and the corresponding processes are the C_3-symmetric and D_{2d} twisted line scatterings as seen for monopoles in Chapter 8. The Skyrmion collision for the first of these has already been described earlier in this section and the twisted line scattering is described in ref. [40]. For $B = 2$, the monopole mode separates the two Skyrmions and the corresponding collision process is right-angle scattering.

In summary, we see that there is a strong correlation between the low-lying vibrational modes of a Skyrmion and the zero modes of the associated monopole. An analysis of rational maps clarifies the correlation. Furthermore, an extension of these modes to large amplitude shows a correspondence between monopole dynamics, studied within the geodesic approximation, and attractive channel Skyrmion scattering, which has been confirmed using full field simulations. These results suggest that a $(4B + 2)$-dimensional moduli space of Skyrme fields, which includes the nine exact zero modes of a general Skyrmion, may model low energy Skyrmion dynamics. However, no precise construction of a suitable manifold of Skyrme fields directly from rational maps, or from monopole fields, has yet been achieved.

9.9 Generalizations of the Skyrme model

In arriving at the Skyrme model as a low energy effective theory from QCD in the limit in which the number of colours, N_c, is large, one finds that the Skyrme field takes values in $SU(N_f)$, where N_f is the number of flavours of light quarks. So far we have only considered the case of $N_f = 2$, which is physically the most relevant since the up and down quarks are almost massless, and the $SU(2)$ flavour symmetry between up and down quarks is only weakly broken in nature; but the model with

$SU(3)$ flavour symmetry, to allow for the strange quark, with appropriate additional symmetry breaking terms to take account of the higher strange quark mass, is also a reasonable approximation and allows the possibility to study strange baryons and nuclei within the Skyrme model, and also scattering processes involving ordinary baryons and strange mesons. The basic fields (of the linearized model) now describe pions, kaons, and the eta meson. There is still just one topological charge, identified as baryon number, arising from the homotopy group $\pi_3(SU(3)) = \mathbb{Z}$. In the absence of any symmetry breaking mass terms, the three flavour Skyrme Lagrangian is given by the usual expression (9.2), but with $U \in SU(3)$. There is also a Wess-Zumino term, which we discuss below, but this only plays a role in the quantization of Skyrmions and can be ignored for the present discussion of classical solutions.

Obviously, solutions of the $SU(3)$ model can be obtained by a simple embedding of $SU(2)$ Skyrmions, and current evidence suggests that these are the minimal energy solutions at each charge. However, there are also solutions which do not correspond to $SU(2)$ embeddings, and although they have energies which are slightly higher than the embedded Skyrmions, they are still low energy configurations, and they have symmetries that are very different from the $SU(2)$ solutions and so may be of some interest.

An example of a non-embedded solution is the dibaryon of Balachandran *et al.* [30], which is a spherically symmetric solution with $B = 2$. Explicitly, the Skyrme field is given by

$$U(\mathbf{x}) = \exp\left\{ if_1(r)\boldsymbol{\Lambda}\cdot\hat{\mathbf{x}} + if_2(r)\left((\boldsymbol{\Lambda}\cdot\hat{\mathbf{x}})^2 - \frac{2}{3}1_3\right)\right\}, \tag{9.132}$$

where $\boldsymbol{\Lambda}$ is a triplet of $su(3)$ matrices generating $so(3)$ and f_1, f_2 are real profile functions satisfying the boundary conditions $f_1(0) = f_2(0) = \pi$ and $f_1(\infty) = f_2(\infty) = 0$. Substituting this ansatz into the static Skyrme equation leads to two coupled ordinary differential equations for f_1 and f_2. Solving these numerically yields an energy per baryon of $E/B = 1.19$, which is about 1% higher than the energy of the embedded $SU(2)$ torus of charge 2.

Recently, an extension of the rational map ansatz has been proposed [206], to create $SU(N_f)$ Skyrme fields from rational maps of the Riemann sphere into $\mathbb{CP}^{N_f-1}$. Explicitly, the ansatz extends the $SU(2)$ projector form (9.56) to

$$U = \exp\left(if\left(2P - \frac{2}{N_f}1_{N_f}\right)\right), \tag{9.133}$$

where P is now an $N_f \times N_f$ Hermitian projector, constructed from a vector

$\mathbf{v}$ with N_f components via

$$P = \frac{\mathbf{v} \otimes \mathbf{v}^\dagger}{|\mathbf{v}|^2}, \tag{9.134}$$

and $f(r)$ is a real radial profile function with the usual boundary conditions. The vector $\mathbf{v}(z) : S^2 \mapsto \mathbb{CP}^{N_f-1}$ appears to be a rational map from the Riemann sphere into $\mathbb{C}^{N_f}$, but it is only defined projectively due to the relation (9.134). In fact, we can use this projective property to take $\mathbf{v}$ to be a vector in which all components are polynomials in z, and the degree of this projector, which is equal to the baryon number of the resulting Skyrme field, is given by the highest degree of the component polynomials. When $N_f = 2$ this ansatz coincides with the usual $SU(2)$ ansatz after the identification $\mathbf{v} = (q, p)^t$, where $R = p/q$ is the usual rational map and we have made use of the equivalence $\mathbb{CP}^1 \cong S^2$.

Although there are some difficulties with this ansatz [394], it can be used to produce some low energy field configurations and to understand the existence of certain symmetric Skyrme fields, which do not exist at the same charge in the $SU(2)$ model.

The $SU(N_f)$ Skyrme model has a global $SU(N_f)/\mathbb{Z}_{N_f}$ symmetry corresponding to the conjugation $U \mapsto \mathcal{O}U\mathcal{O}^\dagger$, where $\mathcal{O} \in SU(N_f)$. In terms of the ansatz (9.133) this symmetry is represented by the target space transformation

$$\mathbf{v} \mapsto \mathcal{O}\mathbf{v}. \tag{9.135}$$

The identification of K-symmetric maps (and hence K-symmetric Skyrme fields) is analogous to the $SU(2)$ case. The set of target space rotations accompanying spatial rotations needs to form an N_f-dimensional representation of K, so the simplest situation in which a degree B symmetric map exists is when

$$\underline{B+1}|_K = X_{N_f} \oplus \cdots, \tag{9.136}$$

where $\underline{B+1}|_K$ is the restriction of the $(B+1)$-dimensional irreducible representation of $SU(2)$ to the subgroup K, and X_{N_f} denotes any N_f-dimensional irreducible representation of K. In this case a basis for X_{N_f} consists of N_f polynomials in z of degree B, which can be taken to be the N_f components of the vector $\mathbf{v}$.

To illustrate these ideas let us consider $B = 6$ Skyrme fields with icosahedral symmetry in the $SU(3)$ model. The relevant decomposition is

$$\underline{7}|_Y = F_2 \oplus G. \tag{9.137}$$

The presence of the three-dimensional F_2 shows that there is an icosahedrally symmetric degree 6 map from $\mathbb{CP}^1$ into $\mathbb{CP}^2$. Explicitly, this map is given by

$$\mathbf{v}(z) = (z^6 + 3z,\ 1 - 3z^5,\ \sqrt{50}z^3)^t \tag{9.138}$$

and is Y_h-symmetric. Thus there is an icosahedrally symmetric $B = 6$ Skyrme field in the $SU(3)$ model, whereas, as we have seen earlier, the lowest charge for which there is an icosahedrally symmetric $SU(2)$ Skyrmion is $B = 7$.

Substituting the ansatz (9.133) into the Skyrme Lagrangian leads to an energy function on the space of rational maps into $\mathbb{CP}^{N_f-1}$, and an essentially independent energy function for the profile function. In the case of $N_f = 3$ and $B = 6$ a numerical search for the minimizing map produces the map above [206], suggesting that the minimal energy non-embedded $SU(3)$ Skyrmion of charge 6 may be Y_h-symmetric. The profile function is also easily determined numerically. Numerical investigations of the full $SU(3)$ Skyrme model need to be performed to find the precise solutions of lowest energy, but this has yet to be done.

We now turn to a different generalization, the Skyrme model on a 3-sphere, in which the domain $\mathbb{R}^3$ is replaced by S^3_L, the 3-sphere of radius L, but the Skyrme field is still a map to the target space $SU(2)$. The baryon number is the degree of U. This generalization has been studied in ref. [291], and in a more geometrical context in ref. [282], where it was also shown that the geometrical strain formulation discussed earlier can be used to define a Skyrme energy functional for a map between any three-dimensional Riemannian manifolds. By taking the limit $L \to \infty$ the Euclidean model is recovered, but it is possible to gain some additional understanding of Skyrmions by first considering finite values of L.

Let μ, z be coordinates on S^3_L, with μ the polar angle (the co-latitude) and z the Riemann sphere coordinate on the 2-sphere at polar angle μ. Take f, R to be similar coordinates on the unit 3-sphere S^3_1, which we identify with the target manifold $SU(2)$.

In general, a static field is given by functions $f(\mu, z, \bar{z})$ and $R(\mu, z, \bar{z})$, but various simplifications are possible. To find the $B = 1$ Skyrmion we consider an analogue of the hedgehog field, an $SO(3)$-symmetric map of the form

$$f = f(\mu), \quad R = z, \tag{9.139}$$

whose energy is

$$E = \frac{1}{3\pi}\int_0^\pi \left\{ L\sin^2\mu\left(f'^2 + \frac{2\sin^2 f}{\sin^2\mu}\right) + \frac{\sin^2 f}{L}\left(\frac{\sin^2 f}{\sin^2\mu} + 2f'^2\right)\right\} d\mu . \tag{9.140}$$

Among these maps there is the 1-parameter family of degree 1 conformal maps

$$\tan\frac{f}{2} = e^a \tan\frac{\mu}{2}, \tag{9.141}$$

where a is a real constant. These may be pictured as a stereographic projection from S^3_L to $\mathbb{R}^3$, followed by a rescaling by e^a, and then an in-

verse stereographic projection from $\mathbb{R}^3$ to S^3_1. Substituting the expression (9.141) into the energy (9.140), and performing the integral gives

$$E = \frac{L}{1+\cosh a} + \frac{\cosh a}{2L}\,. \tag{9.142}$$

If $a = 0$ then (9.141) is the identity map with energy

$$E = \frac{1}{2}\left(L + \frac{1}{L}\right). \tag{9.143}$$

Note that if $L = 1$ then $E = 1$, so the Faddeev-Bogomolny bound is attained. We can therefore be certain that, in this case, the $B = 1$ Skyrmion is given by the identity map. We mentioned earlier that the bound could only be attained by a mapping which is an isometry, and this occurs when $L = 1$, the domain then being isometric to the target space.

Computing a to minimize the energy (9.142), for a fixed, general value of L, results in

$$\cosh a = \sqrt{2}L - 1\,. \tag{9.144}$$

For $L < \sqrt{2}$ this is clearly unattainable, and in fact the minimum occurs at $a = 0$. This shows that, for $L < \sqrt{2}$, the identity map is stable with respect to conformal transformations, though actually a stronger result, that the identity map is stable against any deformation for $L < \sqrt{2}$, is true [282]. The identity map is thus very likely the Skyrmion. The energy density of the identity map is distributed evenly over the 3-sphere, so no point of either the domain or target spheres is singled out as special. The unbroken symmetry group is the diagonal $SO(4)$ subgroup of the full symmetry group, which may be interpreted either as spatial or chiral $SO(4)$ rotations.

For $L > \sqrt{2}$ there are two roots of equation (9.144), related by the symmetry $a \mapsto -a$, but they give geometrically equivalent solutions since this sign change can be undone by making the replacement $\mu \mapsto \pi - \mu$, which exchanges poles on S^3_L. The energy is

$$E = \sqrt{2} - \frac{1}{2L}\,, \tag{9.145}$$

which is clearly less than (9.143). If a is positive, there is a preferred point in S^3_L, which corresponds to the point at infinity in $\mathbb{R}^3$, where the energy density is minimal, and the image of this point is a preferred point in S^3_1. The unbroken symmetry is therefore $SO(3)$ isospin symmetry, as in the Euclidean case, and chiral symmetry is broken. The energy density is maximal at the antipodal point. These conformal maps are not the exact Skyrmion solutions for $L > \sqrt{2}$, but they are expected to be close.

and have the same symmetry. In the Euclidean limit $L \to \infty$ the radial variable should be identified as the combination $r = L\mu$, in which case the expression for the energy (9.140) reproduces the result for the hedgehog profile function (9.22). In the limit, the conformal map with $e^a \sim \sqrt{8}L$, that is, $f(r) = 2\tan^{-1}(\sqrt{2}r)$, has energy $E = \sqrt{2}$, which is higher than the value $E = 1.232$ of the minimizing hedgehog profile function, but the Skyrme field is qualitatively similar.

In summary, we see that on a small 3-sphere the energy density of a $B = 1$ Skyrmion is uniformly distributed over S^3_L and the unbroken symmetry group is $SO(4)$, but as the radius of the 3-sphere is increased beyond the critical value $L = \sqrt{2}$ there is a bifurcation to a Skyrmion localized around a point and chiral symmetry is broken. Thus a phase transition occurs, as in the Skyrme crystal, when one moves from conditions of high to low baryon density, with a corresponding breaking of chiral symmetry. This may have relevance to the physical issue of whether quark confinement occurs at the same time as chiral symmetry breaking as very dense quark matter becomes less dense.

For charge $B > 1$ the rational map ansatz can again be applied to produce low energy Skyrme fields which approximate the minimal energy Skyrmions on S^3_L [246], by taking $R(z)$ to be a degree B rational map and $f(\mu)$ the associated energy minimizing profile function. This produces fields which tend to those of the Euclidean model as $L \to \infty$ and for all cases except $B = 2$, this ansatz produces the lowest energy configurations yet discovered. The energy is particularly low if one chooses the optimal value of L, which depends on B. For $B = 2$ an exact solution is known [219] which has lower energy than the $O(2)$ symmetric field obtained from the rational map ansatz with $R = z^2$. This solution has a doubly axially symmetric form with the larger symmetry $O(2) \times O(2)$, a subgroup of the $O(4)$ symmetry group of the 3-sphere Skyrme model that is lost in the Euclidean limit.

Finally, in introducing the Skyrme model in Section 9.1 we already mentioned that a possible modification of the model is the addition of the pion mass term (9.7). The qualitative results of our previous discussions are unchanged by its inclusion, but here we briefly mention the small quantitative differences it generates. The most important effect is that the Skyrmion becomes exponentially localized, in contrast to the algebraic asymptotic behaviour of the Skyrme field in the massless pion model. This is because the modified equation for the hedgehog profile function,

$$(r^2 + 2\sin^2 f)f'' + 2rf' + \sin 2f\left(f'^2 - 1 - \frac{\sin^2 f}{r^2}\right) - m_\pi{}^2 r^2 \sin f = 0\,, \tag{9.146}$$

has the asymptotic Yukawa-type solution

$$f(r) \sim \frac{A}{r} e^{-m_\pi r} . \tag{9.147}$$

Clearly the energy of a single Skyrmion with $m_\pi > 0$ will be slightly higher than with $m_\pi = 0$, because the pion mass term is positive for all fields. For higher charge Skyrmions, the rational map approach works as before, but the profile function will again be slightly modified, leading to slightly higher energies.

9.10 Quantization of Skyrmions

Quantization is a vital issue for Skyrmions, more so than for the other solitons we have discussed, because Skyrmions are supposed to model physical baryons and nuclei, and a single baryon is a spin half fermion. We consider here both the $SU(2)$ and $SU(N_f)$ Skyrme models in $\mathbb{R}^3$.

We first briefly discuss the Wess-Zumino term [424], which is an additional contribution to the action of the $SU(N_f)$ Skyrme model given by

$$S_{WZ} = -\frac{iN_c}{240\pi^2} \int \varepsilon^{\mu\nu\alpha\beta\gamma} \mathrm{Tr}(R_\mu R_\nu R_\alpha R_\beta R_\gamma)\, d^5x , \tag{9.148}$$

where the integration is performed over a five-dimensional region whose boundary is four-dimensional space-time. The Wess-Zumino term does not contribute to the classical energy, but it plays an important role in the quantum theory. Its introduction breaks the time reversal and parity symmetries of the model down to the combined symmetry operation

$$t \mapsto -t , \quad \mathbf{x} \mapsto -\mathbf{x} , \quad U \mapsto U^\dagger , \tag{9.149}$$

which appears to be realized in nature, unlike these individual symmetry operations. A topological argument shows that N_c must be an integer, and Witten [428] argued that it should be identified with the number of quark colours, based on considerations of flavour anomalies in the quark and Skyrme models.

To determine whether a Skyrmion should be quantized as a fermion we can compare the amplitudes for the processes in which a Skyrmion remains at rest for some long time T, and in which the Skyrmion is slowly rotated through an angle 2π during this time. The sigma model and Skyrme terms in the action do not distinguish between these two processes, since they involve two or more time derivatives, but the Wess-Zumino term is only linear in time derivatives and so can distinguish them. In fact it results in the amplitudes for these two processes differing by a

factor $(-1)^{N_c}$, which shows that the Skyrmion should be quantized as a fermion when N_c is odd, and in particular, in the physical case $N_c = 3$ [428].

For $N_f = 2$ the above analysis does not apply, since the Wess-Zumino term vanishes for an $SU(2)$-valued field. To determine the appropriate quantization of an $SU(2)$ Skyrmion one may follow the approach of Finkelstein and Rubinstein [132], who showed that it is possible to quantize a soliton as a fermion by lifting the classical configuration space to its simply connected covering space. In the $SU(2)$ Skyrme model, this is a double cover for any value of B. To treat a single soliton as a fermion, states should be multiplied by a factor of -1 when acted upon by any operation corresponding to a circuit around a non-contractable loop in the configuration space. Equivalently, the wavefunction has opposite signs on the two points of the covering space that cover one point in the configuration space. These authors also showed that the exchange of two $B = 1$ Skyrmions is a loop which is homotopic to a 2π rotation of a Skyrmion, in agreement with the spin-statistics result. It was verified by Williams [426] that a 2π rotation of a single Skyrmion is a non-contractible loop, thus requiring the Skyrmion to be quantized as a fermion. This result was generalized by Giulini [154], who showed that a 2π rotation of a charge B Skyrmion is a non-contractible loop if B is odd and contractible if B is even.

A practical, approximate quantum theory of Skyrmions is achieved by a rigid body quantization of the spin and isospin rotations. Vibrational modes whose excited states usually have considerably higher energy are ignored. For the $B = 1$ Skyrmion, this quantization was carried out by Adkins, Nappi and Witten [7], who showed that the lowest energy states (compatible with the Finkelstein-Rubinstein constraints) have spin half and isospin half, and may be identified with states of a proton or neutron.

The quantization of the $B = 2$ Skyrmion was first discussed by Braaten and Carson [64], using a rigid body quantization. Their analysis was extended by Leese, Manton and Schroers [261], who also allowed the toroidal Skyrmion to break up in the direction of the lowest vibrational mode, which corresponds to the attractive channel. Both calculations find that the lowest energy quantum state has isospin zero and spin 1, as expected for the deuteron. The second calculation gets closer to the usual physical picture of the deuteron as a rather loose proton-neutron bound state.

For higher charge Skyrmions symmetric under a discrete group K, the moduli space of zero modes is $(SO(3) \times SO(3))/K$, where in this case K really denotes the group and not its double cover. K can be replaced

by its double cover, K', if the $SO(3)$ factors in the above quotient space are promoted to $SU(2)$. A quantization of the zero modes can be performed by quantizing on this quotient space, but there are a number of inequivalent ways to do this labelled by the irreducible representations of K'. It is most convenient to define the wavefunctions on $SU(2) \times SU(2)$, and require them to be eigenstates of the operations corresponding to the elements of K'. The Finkelstein-Rubinstein constraints are imposed by requiring the eigenvalues to be ± 1 depending on whether the particular element of K' corresponds to a contractible or non-contractible loop. This has been performed [64, 74, 411, 210] for charges $B \leq 8$, and gives the correct quantum numbers (spin, isospin and parity) for the experimentally observed ground states of nuclei in all cases except $B = 5$ and $B = 7$. A further study, making use of the topological properties of the space of rational maps, has allowed an extension of this analysis up to $B = 22$ [247]. The fact that some results do not agree with the experimental data is probably due to the restricted zero mode quantization, which does not allow any vibrational or deformation modes, and assumes a rigid rotor approximation so that the symmetry of the static solution is maintained even in the presence of spin.

9.11 The Skyrme-Faddeev model

Some time ago, Faddeev [125] suggested that stable closed strings may exist as topological solitons in a modified $O(3)$ sigma model which includes a fourth order derivative term, with the topology arising due to the twisting of a planar soliton along the length of the string. Each slice normal to the string carries the localized planar soliton. The Skyrme-Faddeev model, which realizes this idea, involves a map $\mathbf{n} : \mathbb{R}^3 \mapsto S^2$, and can be obtained from the Skyrme model simply by restricting the field values to an equatorial 2-sphere of the usual $SU(2)$ target space. Explicitly, the field of the model is a real three-component vector $\mathbf{n} = (n_1, n_2, n_3)$, with unit length, $\mathbf{n} \cdot \mathbf{n} = 1$. The associated restricted Skyrme field is $U = i\mathbf{n} \cdot \boldsymbol{\tau}$. Substituting this into the Skyrme Lagrangian (9.2) results in

$$L = \int \left\{ \partial_\mu \mathbf{n} \cdot \partial^\mu \mathbf{n} - \frac{1}{2} (\partial_\mu \mathbf{n} \times \partial_\nu \mathbf{n}) \cdot (\partial^\mu \mathbf{n} \times \partial^\nu \mathbf{n}) \right\} d^3x , \qquad (9.150)$$

which is the Skyrme-Faddeev Lagrangian. Its first term is that of the $O(3)$ sigma model and the higher order derivative Skyrme term is, as usual, required to give the possibility of configurations which are stable under a spatial rescaling.

In order for a field configuration to have finite energy the vector $\mathbf{n}$ must tend to a constant value at spatial infinity, which we may take to

be the vector $\mathbf{n}^\infty = (0,0,1)$. Finite energy field configurations have a topological classification, but the novel aspect of this model is that the topological charge is not a topological degree, as it is for the solitons we have considered so far in this book, such as vortices, monopoles or Skyrmions.

The boundary condition again compactifies space to S^3, so that at any given time the field is a map $\mathbf{n} : S^3 \mapsto S^2$. Since $\pi_3(S^2) = \mathbb{Z}$, there is an associated integer topological charge N, the Hopf charge, which gives the soliton number. This charge can not be the degree of the mapping, since the domain and target spaces have different dimensions. Instead, one definition is the following. Let ω denote the area 2-form on the target S^2 and let $f = \mathbf{n}^*\omega$ be its pull-back under $\mathbf{n}$ to the domain S^3. Since ω is closed, f is closed. Then, due to the triviality of the second cohomology group of the 3-sphere, $H^2(S^3) = 0$, this pull-back must be an exact 2-form, say $f = da$. The Hopf charge is constructed by integrating the Chern-Simons 3-form over S^3,

$$N = \frac{1}{4\pi^2}\int_{S^3} f \wedge a\,. \tag{9.151}$$

This integral is independent of the choice of a, because if $a \mapsto a + d\alpha$, then the change of N is

$$\Delta N = \frac{1}{4\pi^2}\int_{S^3} f \wedge d\alpha = \frac{1}{4\pi^2}\int_{S^3}(d(f\alpha) - (df)\alpha) = 0 \tag{9.152}$$

because $df = 0$, and by Stokes' theorem the integral of $d(f\alpha)$ vanishes over a closed 3-manifold.

An important point to note is that the Hopf charge can not be written as the integral of any density which is local in the field $\mathbf{n}$. For this reason it is useful to consider an alternative interpretation of N. Generically, the preimage of a point on the target S^2 is a closed loop in S^3. Now if a field has Hopf number N then the two loops consisting of the preimages of any two distinct points on the target S^2 will be linked exactly N times. In Fig. 9.12 we schematically represent the preimages of two points for a configuration with $N = 1$.

Solitons have been found in the Skyrme-Faddeev model for a range of values of N. They are string-like, but not all of a simple shape. Recall that the position of a lump or Skyrmion is sometimes defined to be the point in space at which the field takes the value antipodal to the vacuum value. Here, the position of a soliton is the curve in space which is the preimage of the vector $-\mathbf{n}^\infty = (0,0,-1)$. Displaying this closed string is a useful way to represent the solution. Alternatively, a thickened version of the soliton may be represented by the preimage of the circle of vectors with $n_3 = \text{const}$. The Skyrme-Faddeev model has a global $O(3)$ symmetry, but

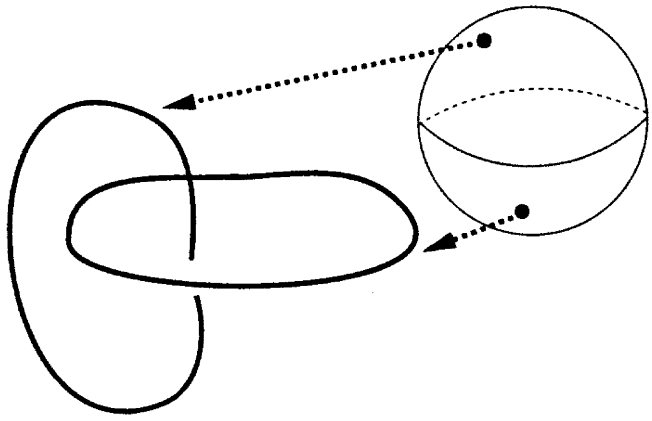

Fig. 9.12. A sketch showing two loops corresponding to the preimages of two points on the target 2-sphere. The loops are linked exactly once, indicating that the configuration has Hopf charge $N = 1$.

the choice of a vacuum value $\mathbf{n}^{\infty}$ breaks this to an $O(2)$ symmetry, which rotates the (n_1, n_2) components. As usual, when we refer to a symmetry of a configuration we mean that the effect of a spatial transformation can be undone by acting with an element of the unbroken global symmetry group of the theory, in this case $O(2)$. This implies that both the n_3 component (which determines the position of the soliton) and the energy density are strictly invariant under the symmetry operation.

Not only is there a topological Hopf charge in this model, but there is also a lower bound on the energy in terms of the charge N [405, 249]. Explicitly,

$$E > c|N|^{3/4} \tag{9.153}$$

where $c = 16\pi^2 3^{3/8} \approx 238$. This energy bound is rather unusual in that a fractional power of the topological charge occurs, reflecting the fact that this bound is not obtained from the usual Bogomolny-type argument, but relies on a sophisticated use of Sobolev inequalities for its derivation. As such, the above value for the constant c may not be very tight. We will comment further on this shortly.

As pointed out in ref. [405], spherically symmetric fields automatically have zero Hopf charge, so it is not immediately obvious how to write down even the simplest field configurations which have non-zero values of N. However, a toroidal field can be constructed for any N, based on Faddeev's original idea. One may think of this field as a two-dimensional Baby Skyrmion which is embedded in the normal slice to a circle in space

and has its internal phase rotated through an angle $2\pi N$ as it travels around the circle once. The construction can be implemented in toroidal coordinates if the size of the circle is fixed in advance, and was the method used in the numerical investigations [127, 155], which established the existence of axially symmetric solitons with charges $N = 1$ and $N = 2$, but it is rather cumbersome. A more elegant approach to constructing field configurations with non-zero Hopf charge makes use of the observation [302] that a field with Hopf charge N can be obtained by applying the standard Hopf projection $H : S^3 \mapsto S^2$ to a map U between 3-spheres with winding number N – in other words, a Skyrme field. Precisely, let $U(\mathbf{x})$ be a Skyrme field, that is, any smooth map from $\mathbb{R}^3$ into $SU(2)$ which satisfies the boundary condition that U tends to the identity as $|\mathbf{x}| \to \infty$. Let U have baryon number (degree) B. By writing the matrix entries of U in terms of complex numbers Z_0 and Z_1 as

$$U = \begin{pmatrix} Z_0 & -\bar{Z}_1 \\ Z_1 & \bar{Z}_0 \end{pmatrix}, \tag{9.154}$$

where $|Z_0|^2 + |Z_1|^2 = 1$, the image of the Hopf map H can be written in terms of the column vector $Z = (Z_0, Z_1)^{\mathrm{t}}$ as

$$\mathbf{n} = Z^\dagger \boldsymbol{\tau} Z\,. \tag{9.155}$$

It is easy to see that $\mathbf{n}$ is a real 3-vector of unit length and satisfies the boundary condition $\mathbf{n}(\infty) = \mathbf{n}^\infty$. Furthermore, it can be shown that the Hopf charge of the configuration constructed in this way is equal to the baryon number of the Skyrme field U, that is, $N = B$.

A useful supply of Skyrme fields for this purpose can be obtained using the rational map ansatz, as described in Section 9.5. Recall that this involves a rational map $R(z)$ and profile function $f(r)$. In particular, choosing the map $R(z) = z^N$ gives an axially symmetric field $\mathbf{n}$ of Hopf charge N, which has the same qualitative properties as those constructed by hand using toroidal coordinates. Note that in the case $N = 1$ the Skyrme field is spherically symmetric, but the Hopf projection breaks this, so that the vector $\mathbf{n}$ has only an axial symmetry. To determine the position of any approximate soliton constructed using this method we need to calculate the points in $\mathbb{R}^3$ at which $\mathbf{n} = (0, 0, -1)$. Equation (9.155) shows that this is equivalent to finding where $Z_0 = 0$. In the rational map ansatz, $Z_0 = 0$ if $f(r) = \frac{1}{2}\pi$ and also $|R(z)| = 1$. For the family of maps $R = z^N$ the second condition gives $|z| = 1$, the equatorial circle on the Riemann sphere. Therefore the position of the soliton is a circle in the (x^1, x^2) plane, whose radius is determined by the first condition.

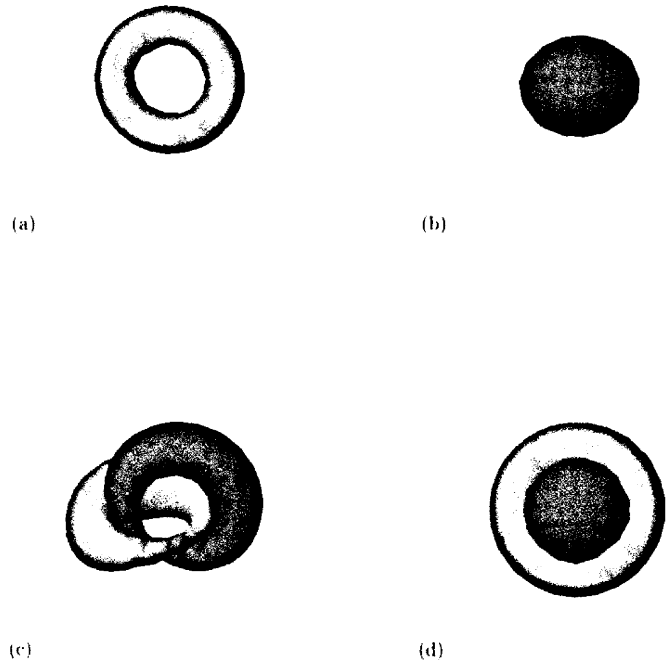

Fig. 9.13. Isosurface plots for the $N = 1$ soliton displaying (a) the thickened locus of the position, (b) the energy density, (c) linking structure between two independent points on the target 2-sphere, and (d) a comparison between the position and energy density. Notice that the linking number is indeed 1 and that the energy density is not toroidal, but rather its maximum occurs at a point inside the locus of the position.

Using these axially symmetric configurations as initial data in a full three-dimensional numerical relaxation [43], it is found that for $N = 1$ and $N = 2$ the minimal energy soliton fields are very close to the initial data. In Fig. 9.13 and Fig. 9.14 we present, for the $N = 1$ and $N = 2$ solitons respectively, the position, the energy density, the linking number (by plotting the preimages of the points $\mathbf{n} = (-1, 0, 0)$ and $\mathbf{n} = (0, -1, 0)$). and the position and energy density isosurface together for comparison.

The energy of the $N = 1$ soliton has been computed several times [155, 43, 179, 419], using a variety of numerical schemes, and within the accuracy of the numerical calculations it is $E \approx 545$. Note that this is more than double the bound (9.153) with the quoted value of c, in agreement with our earlier remark that this value is probably not optimal. Ward [418] has argued (but it has not yet been proven) for the stronger value

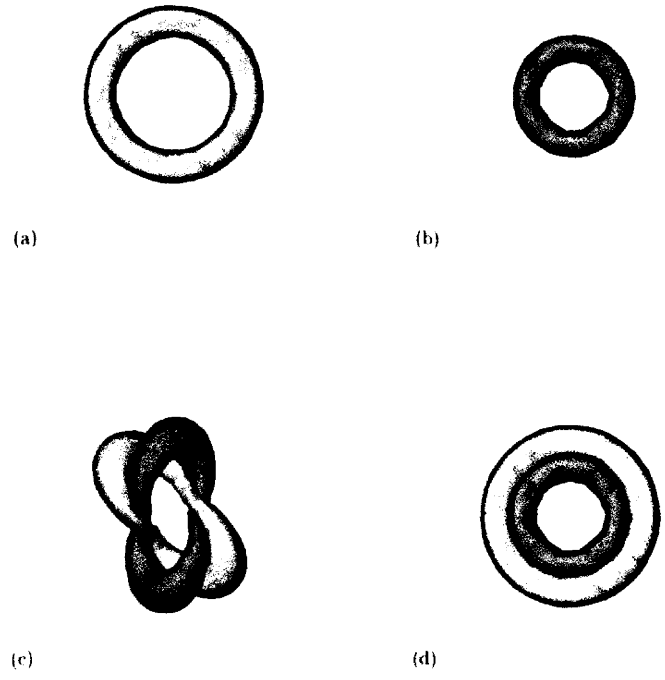

Fig. 9.14. The same quantities as in Fig. 9.13, but for the $N = 2$ soliton. Notice that the locus of the position and the energy density are both toroidal, but that the energy density is peaked inside the position.

$c = 32\pi^2\sqrt{2} \approx 447$. This is better from the point of view of the $N = 1$ soliton, since its energy would then only exceed the bound by roughly 20%, as would the energies of the higher charge solitons [43]. Ward's value is arrived at by considering the Skyrme-Faddeev model on S^3_L rather than $\mathbb{R}^3$, in analogy with the discussion of Skyrmions on a 3-sphere. As in the Skyrme model, there is a special radius of the sphere, in this case[†] $L = \sqrt{2}$, for which an exact solution can be obtained, which corresponds to the identity map from S^3_L to S^3_1 followed by the standard Hopf projection. The energy of this solution, which is possibly an absolute minimum for a soliton of unit charge, is precisely the value of c proposed by Ward. Thus if the Skyrme-Faddeev model mimics the result in the Skyrme model, where the topological energy bound is attained at the special radius, and is otherwise exceeded, then this energy is a natural candidate for the optimal constant c. Other aspects of the Skyrme model on a 3-sphere also

[†] The fact that the special radius is not $L = 1$ is simply due to our choice of coefficients in front of the two terms in the Lagrangian (9.150).

find parallels in the Skyrme-Faddeev model. For example, the identity map followed by the Hopf projection is an unstable solution if the radius L exceeds a critical value, which in the normalization we have chosen is $L > 2$.

Returning to solitons of the Skyrme-Faddeev model in flat space, for $N > 2$ the results of the numerical relaxation show that the minimal energy solution does not have the axially symmetric form described above. For example, the position of the $N = 3$ soliton has the structure of a twisted loop; this is displayed in the first plot of Fig. 9.15. Faddeev

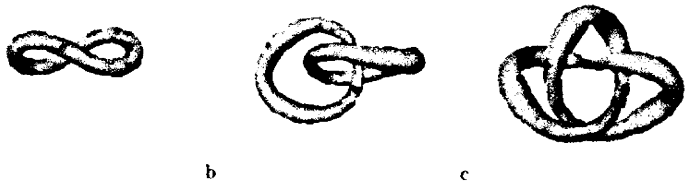

Fig. 9.15. The position of the soliton for (a) $N = 3$, (b) $N = 6$, (c) $N = 7$.

and Niemi [127] conjectured that the string-like solitons in this model would form knotted configurations for large enough values of N. This was verified numerically in ref. [43] (and later in ref. [179]) where both links and knots were found as the minimal energy solutions at various Hopf charges. The second and third plots of Fig. 9.15 show the position of the soliton for $N = 6$ and $N = 7$. The $N = 7$ soliton has the form of a trefoil knot, while the $N = 6$ soliton is composed of two linked loops which each resemble the $N = 2$ soliton. The total Hopf charge is here $N = 6$ because there is an additional two units of charge associated with the double counting of the linking number of two preimages, when the preimage of a single point itself has disconnected, linked components. The fact that the linking number is not simply additive, as this example demonstrates, is probably the physical reason why the energy bound (9.153) grows slowly, as a fractional power of the Hopf charge N.

As with Skyrmions, it is expected that the configuration space of the Skyrme-Faddeev model is very complicated, leading to many solutions which are local energy minima but not global minima, in addition to saddle point solutions. In fact, because of the string-like nature of the solutions, it is very likely that the difficulties associated with finding the global minimum at each charge will be much worse than in the Skyrme model. It has already been demonstrated [419] that even the space of $N = 2$ field configurations has quite a complicated structure.

Further numerical and analytical studies are required to fully investigate the soliton solutions which are expected to exist for higher Hopf

charge, and to determine whether more complicated knots and links arise as the minimal energy solutions. There is physical motivation for this, since it has been proposed that the Skyrme-Faddeev model arises as a dual description of strongly coupled $SU(2)$ Yang-Mills theory [128], with the solitonic strings possibly representing glueballs.

Finally, we note that in the model with Lagrangian

$$L = \int \{(\partial_\mu \mathbf{n} \times \partial_\nu \mathbf{n}) \cdot (\partial^\mu \mathbf{n} \times \partial^\nu \mathbf{n})\}^{3/4} \, d^3x \,, \tag{9.156}$$

exact solutions describing axially symmetric Hopf solitons can be found explicitly [12]. This rather strange model, involving a fractional power in the Lagrangian density, is scale invariant. The solitons are therefore similar to lumps in the $O(3)$ sigma model, in that they have a zero mode associated with changes in the scale of the soliton, which might lead to soliton collapse in a finite time in dynamical situations.